HEALTH AND MEDICINE

Ionizable lipid nanoparticles for in utero mRNA delivery

Rachel S. Riley[1]*, Meghana V. Kashyap[2]*, Margaret M. Billingsley[1]*, Brandon White[2], Mohamad-Gabriel Alameh[3], Sourav K. Bose[2], Philip W. Zoltick[2], Hiaying Li[2], Rui Zhang[1], Andrew Y. Cheng[2], Drew Weissman[3], William H. Peranteau[2†], Michael J. Mitchell[1,4,5,6,7†]

Clinical advances enable the prenatal diagnosis of genetic diseases that are candidates for gene and enzyme therapies such as messenger RNA (mRNA)–mediated protein replacement. Prenatal mRNA therapies can treat disease before the onset of irreversible pathology with high therapeutic efficacy and safety due to the small fetal size, immature immune system, and abundance of progenitor cells. However, the development of nonviral platforms for prenatal delivery is nascent. We developed a library of ionizable lipid nanoparticles (LNPs) for in utero mRNA delivery to mouse fetuses. We screened LNPs for luciferase mRNA delivery and identified formulations that accumulate within fetal livers, lungs, and intestines with higher efficiency and safety compared to benchmark delivery systems, DLin-MC3-DMA and jetPEI. We demonstrate that LNPs can deliver mRNAs to induce hepatic production of therapeutic secreted proteins. These LNPs may provide a platform for in utero mRNA delivery for protein replacement and gene editing.

INTRODUCTION

Advances in DNA sequencing technology and prenatal diagnostics, including the ability to detect cell-free fetal DNA in maternal circulation, allow for the diagnosis of many genetic diseases before birth (*1*, *2*). Some of these congenital diseases are currently managed by protein or enzyme replacement therapies after birth and are prime candidates for gene replacement and/or gene editing approaches. Although postnatal therapy is promising for many diseases, the pathology of some diseases begins before birth and is irreversible, resulting in prenatal or perinatal death or long-term morbidity (*3*). Prenatal therapy enables treatment before the onset of, or in the early stages of, irreversible pathology to significantly reduce disease morbidity and mortality (*4*–*7*). For example, the onset of irreversible disease pathology in some lysosomal conditions begins before birth, and the congenital hematologic disease α-thalassemia can be associated with hemoglobin Bart's hydrops fetalis resulting in prenatal or early postnatal death (*3*, *8*, *9*). Furthermore, glycogen storage diseases and those caused by protein deficiencies are ideal candidates for prenatal therapy (*10*–*14*). Delivering therapeutic nucleic acids or proteins before birth has additional advantages based on the normal ontogeny of the fetus. For example, the small fetal size allows for the administration of a maximal therapeutic dose per recipient weight (*6*). Furthermore, target progenitor cells in multiple organs are more prevalent and highly accessible during gestation, and many physical barriers, such as the blood-brain barrier, are not as developed as they are after birth (*7*, *15*). Finally, prenatal delivery of nucleic acids may induce immunologic tolerance to the therapeutic protein due to the tolerogenic nature of the fetal immune system (*16*, *17*).

Protein and enzyme replacement therapy could occur via direct protein delivery or nucleic acid delivery (*10*, *12*). Therapeutic protein replacement via mRNA delivery has several potential benefits over delivery of other types of nucleic acids, such as DNA, and whole proteins. For example, unlike DNA, mRNA induces transient protein expression in the cytosol, avoiding the need for nuclear entry without risk of genome integration (*18*). Unlike direct delivery of proteins, the use of endogenous machinery to produce the therapeutic protein following mRNA delivery allows for natural posttranslational modifications to occur (*14*). However, similar to known delivery barriers in adults, the implementation of mRNA therapeutics for in utero therapy is met with several limitations including mRNA instability leading to rapid degradation and poor cellular uptake due to the negative charge of naked mRNA (*19*, *20*). These limitations preclude the clinical use of nucleic acids, including mRNA, in both pre- and postnatal disease management, making it necessary to develop novel mRNA delivery technologies (*21*, *22*).

Common methods for therapeutic nucleic acid delivery include viral- and nonviral-mediated approaches (*4*, *5*, *23*, *24*). Although viral-mediated delivery of nucleic acids for gene therapy, including prenatal gene therapy (*4*, *5*, *23*), holds tremendous promise, nonviral-mediated delivery may be a more suitable alternative (*25*, *26*). Nucleic acid delivery via viral vectors presents the risk of ectopic vector integration, which may lead to persistent transgene expression and deleterious consequences for some therapies including gene editing (*25*, *26*). Alternatively, nonviral mRNA delivery approaches can enable transient nucleic acid expression without the risk of genome integration of the carrier vehicle (*27*). Thus, there is a critical need to develop nonviral and biocompatible nucleic acid delivery technologies to treat prenatal diseases.

The use of nonviral delivery systems has only recently emerged as a technique to enable nucleic acid delivery to fetuses for prenatal therapy (*15*, *28*). Poly(lactic-co-glycolic acid) (PLGA) nanoparticles (NPs) have been shown to induce gene editing in fetal hematopoietic

[1]Department of Bioengineering, University of Pennsylvania, Philadelphia, PA 19104, USA. [2]The Center for Fetal Research, Division of General, Thoracic, and Fetal Surgery, The Children's Hospital of Philadelphia, Philadelphia, PA 19104, USA. [3]Department of Medicine, University of Pennsylvania, Philadelphia, PA 19104, USA. [4]Abramson Cancer Center, Perelman School of Medicine, University of Pennsylvania, Philadelphia, PA 19104, USA. [5]Institute for Immunology, Perelman School of Medicine, University of Pennsylvania, Philadelphia, PA 19104, USA. [6]Cardiovascular Institute, Perelman School of Medicine, University of Pennsylvania, Philadelphia, PA 19104, USA. [7]Institute for Regenerative Medicine, Perelman School of Medicine, University of Pennsylvania, Philadelphia, PA 19104, USA.
*These authors contributed equally to this work.
†Corresponding author. Email: peranteauw@email.chop.edu (W.H.P.); mjmitch@seas.upenn.edu (M.J.M.)

stem cells and mitigate disease in a mouse model of β-thalassemia (*15*). This important study demonstrated the potential of nonviral approaches for nucleic acid delivery to treat congenital diseases while highlighting the need to develop drug delivery technologies specifically for fetal delivery.

The use of PLGA NPs for nucleic acid delivery is supported by several benefits afforded by the NPs including high biocompatibility and biodegradability (*29*). Furthermore, recent studies have advanced techniques of polymeric NP formulation, such as microfluidic devices, which have allowed for precise control over the size of PLGA NPs, overcoming a previous limitation of size control (*29*–*33*). Although PLGA and other polymeric systems hold promise for drug delivery to fetuses, we were interested in developing nonviral, ionizable lipid nanoparticles (LNPs) for this application. LNPs offer small sizes (<100 nm) and yield high cellular uptake, and they have been extensively studied for nucleic acid delivery in adult mice (*19*, *34*, *35*). The use of ionizable lipids also enables endosomal escape for efficient nucleic acid delivery to the cytosol (*36*). Furthermore, LNPs offer the ability to design and evaluate new ionizable polyamine-lipid structures within the LNP formulations to optimize platforms for specific applications such as fetal delivery.

Here, we developed and screened a library of ionizable lipids to create LNPs that enable efficient mRNA delivery to mouse fetuses. In addition to the ionizable lipids, these LNPs contain phospholipids, cholesterol, and lipid anchored poly(ethylene glycol) (PEG) as excipients, which assist in LNP structural integrity, stability, and intracellular mRNA delivery (*35*, *37*, *38*). Each LNP formulation was used to encapsulate mRNA and administered to fetuses through the vitelline vein to evaluate organ distribution and mRNA delivery efficiency (Fig. 1). We demonstrated that several of our LNPs enable functional mRNA delivery to the fetal liver. Furthermore, we identified LNP formulations that also deliver mRNA to the fetal lungs and intestines in addition to the fetal liver. Last, we demonstrate the therapeutic potential of the top LNP designs by using them to deliver erythropoietin (EPO) mRNA. We show that EPO mRNA delivery to hepatocytes in mouse fetuses results in elevated levels of EPO protein in the fetal circulation, which serves as a model for hepatocyte-mediated protein replacement therapy. Collectively, we have developed a prenatal LNP delivery platform for mRNAs that provides a foundation for future treatments including gene and enzyme replacement therapies for prenatally diagnosed genetic diseases.

RESULTS

Characterization of the LNP library

A library of 14 LNPs was prepared as previously described by first synthesizing ionizable lipids using Michael addition chemistry (Figs. 1 and 2A) (*34*). During this process, the polyamine molecules react with the alkyl tails to form the polyamine-lipid cores. The naming convention of LNP formulations throughout this paper reflects both the alkyl tail length (A = C12, B = C14, and C = C16) and the unique polyamine core (labeled numerically 1 to 5) of the ionizable lipid component. For example, LNP A-3 is composed of the C12 epoxide-terminated alkyl tail reacted with the polyamine core labeled "3" in Fig. 2A. These ionizable lipids were then mixed with cholesterol, 1,2-dioleoyl-*sn*-glycero-3-phosphoethanolamine (DOPE) phospholipid, PEG-lipid conjugates, and mRNA via perfusion through microfluidic devices that are designed with herringbone features to induce chaotic mixing (Figs. 1, 2A, and fig. S1) (*39*). In LNPs, the ionizable lipid enables cellular uptake and endosomal escape such that the encapsulated mRNA is delivered to the cytosol (*40*). The excipients (DOPE, cholesterol, and PEG-lipids) were chosen on the basis of previous studies demonstrating that their inclusion yields optimal mRNA delivery in adult mice (*35*). Specifically, DOPE and cholesterol provide stability to the lipid bilayer, enhance mRNA encapsulation, and may assist in endosomal escape (*37*, *38*). The PEG-lipids enhance overall LNP stability and extend circulation (*35*).

LNPs were characterized by size, pK_a, and mRNA encapsulation efficiency (Fig. 2, B and C). The hydrodynamic diameter [by intensity measurements using dynamic light scattering (DLS)] for all LNP formulations ranged from 64.6 to 135.2 nm (Fig. 2C). Only one LNP formulation had a polydispersity (PDI) value above 0.3, with all others having a PDI value less than 0.3, indicating monodisperse LNPs. Each LNP formulation was evaluated for its ability to encapsulate mRNA using RiboGreen assays, and all encapsulation efficiencies were high, ranging from 74 to 97.5% (Fig. 2C). Last, LNPs were assessed for their pK_a, the pH at which the LNPs are 50% protonated. This reflects how pH affects their ability to escape acidic endosomal compartments inside cells (Fig. 2, B and C). pK_a values < 7.0 indicate that the LNPs will become

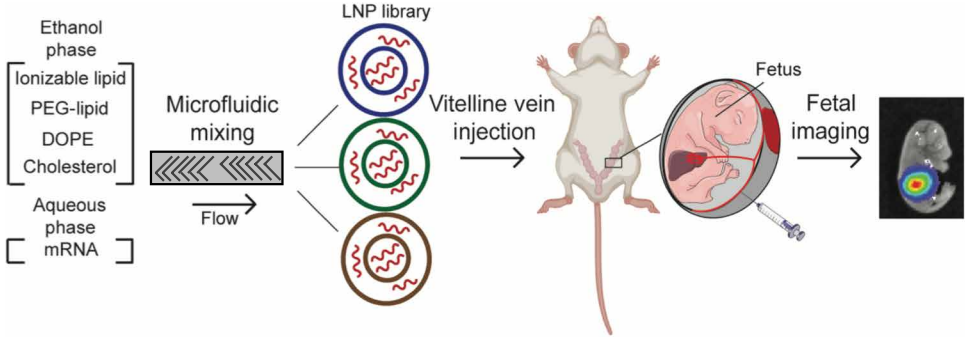

Fig. 1. Overview of LNP formulation and fetal delivery for this study. First, ionizable lipid structures were prepared by Michael addition chemistry. Then, the ionizable lipids, PEG-lipid, DOPE phospholipid, and cholesterol were combined into an ethanol phase, and luciferase mRNA was diluted into an aqueous phase. Both phases were mixed at controlled flow rates in microfluidic devices. After LNP formulation, LNPs were injected to individual mouse fetuses through the vitelline vein, which directly delivers to sinusoids in the fetal liver. After 4 or 24 hours, fetuses and tissues were extracted for imaging and further analysis.

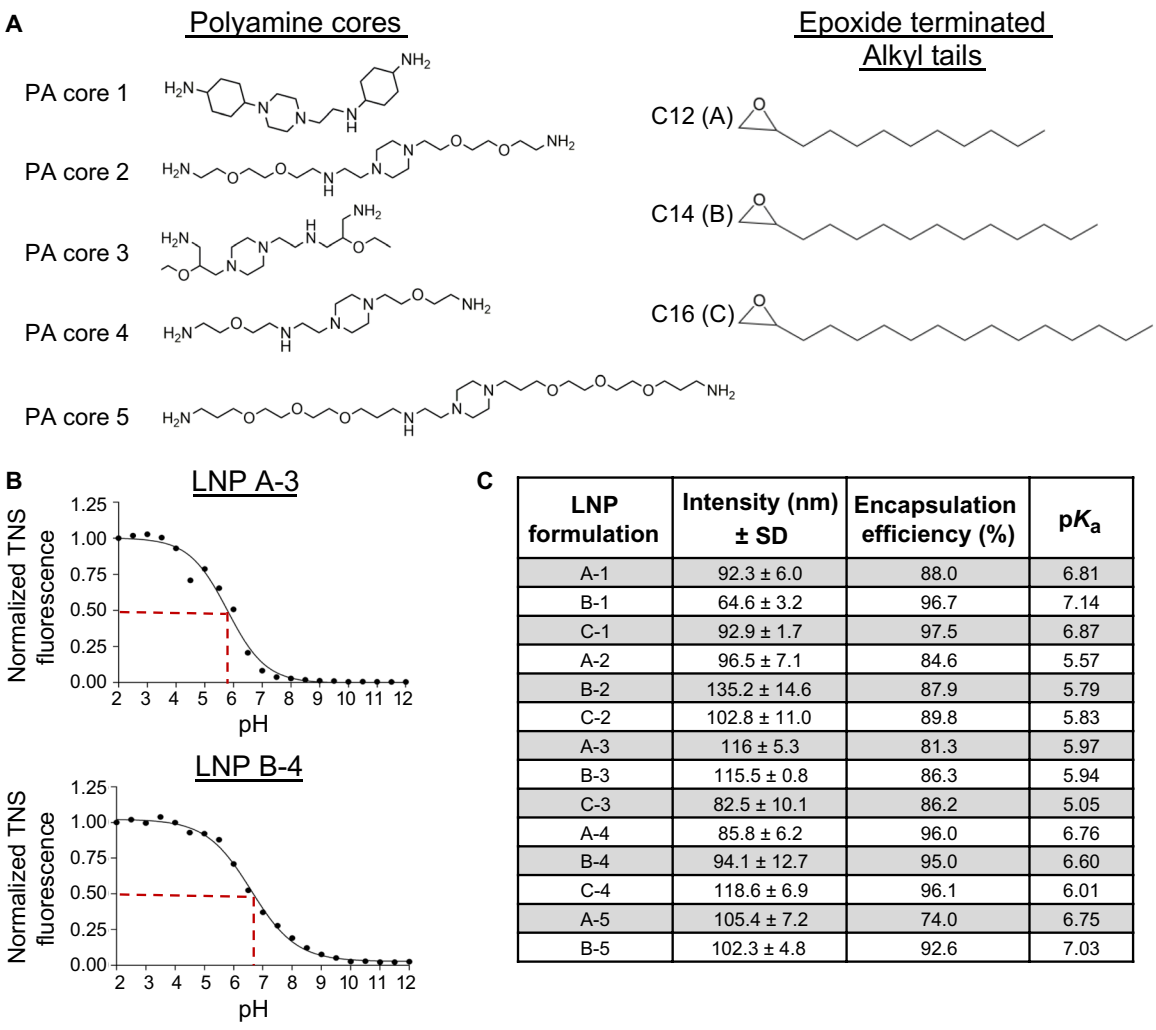

C

LNP formulation	Intensity (nm) ± SD	Encapsulation efficiency (%)	pK_a
A-1	92.3 ± 6.0	88.0	6.81
B-1	64.6 ± 3.2	96.7	7.14
C-1	92.9 ± 1.7	97.5	6.87
A-2	96.5 ± 7.1	84.6	5.57
B-2	135.2 ± 14.6	87.9	5.79
C-2	102.8 ± 11.0	89.8	5.83
A-3	116 ± 5.3	81.3	5.97
B-3	115.5 ± 0.8	86.3	5.94
C-3	82.5 ± 10.1	86.2	5.05
A-4	85.8 ± 6.2	96.0	6.76
B-4	94.1 ± 12.7	95.0	6.60
C-4	118.6 ± 6.9	96.1	6.01
A-5	105.4 ± 7.2	74.0	6.75
B-5	102.3 ± 4.8	92.6	7.03

Fig. 2. Design and characterization of LNPs for fetal mRNA delivery. (**A**) Chemical structures of the polyamine cores (left) and epoxide terminated alkyl tails (right) that were combined to generate the ionizable lipids used in this study. Throughout this paper, LNPs are named for their ionizable lipid component's alkyl tail length (A = C12, B = C14, and C = C16) as well as their polyamine core (numbered 1 to 5). PA, polyamine. (**B**) Graphed analyses of LNP pK_a for representative NPs A-3 and B-4. The pK_a for each LNP was calculated by determining the pH that corresponds to normalized TNS fluorescence at 0.5. (**C**) LNP characterization table showing hydrodynamic diameter (intensity), encapsulation efficiency, and pK_a for each LNP formulation.

protonated in endosomes causing the lipids to fuse with the endosomal membrane for release of mRNA into the cytosol, and pK_a values of 6 to 7 are most commonly reported for in vivo nucleic acid delivery (*36*, *41*, *42*). The measured pK_a values from our LNP library ranged from 5.57 to 7.14, indicating that many of the LNPs were within the desired range for nucleic acid delivery.

LNPs enable in utero mRNA delivery

Next, we evaluated prenatal mRNA delivery via our LNPs using luciferase mRNA, as this system enables direct visualization of transfection efficiency using an in vivo imaging system (IVIS). Thus, detection of luminescence indicates both LNP delivery and mRNA functionality. LNPs encapsulating luciferase mRNA (LNP.luc) were injected into gestational day (E) 16 mouse fetuses (minimum $n = 3$ fetuses per LNP formulation depending on the number of fetuses in each dam) via the vitelline vein, and injected dams and fetuses were assessed by IVIS 4 hours after injection (Figs. 1 and 3A). The vitelline vein drains directly into the fetal portal circulation, so this model represents a midgestation umbilical vein injection in a human fetus. Each mouse fetus has its own gestational sac and vitelline vein such that the vitelline vein injectate of one fetus does not cross over to additional fetuses (*43*). The sample size for each treatment varies because there is a range in the number of fetuses within the uterine horn of each dam. Thus, half of the fetuses in each dam were injected with an LNP formulation while the other half were injected with phosphate-buffered saline (PBS) as an internal negative control for imaging. All of the data shown in Figs. 3 and 4 represent only fetuses injected with LNPs and not the negative PBS-injected controls, none of which demonstrated any signal.

Analysis of pregnant dams following fetal injection revealed strong luciferase signal localized to the fetus for several LNP formulations and no signal in any fetuses injected with PBS (Fig. 3B). In addition, no maternal tissues had luciferase signal, suggesting an absence of transplacental migration of the LNPs from fetus to dam

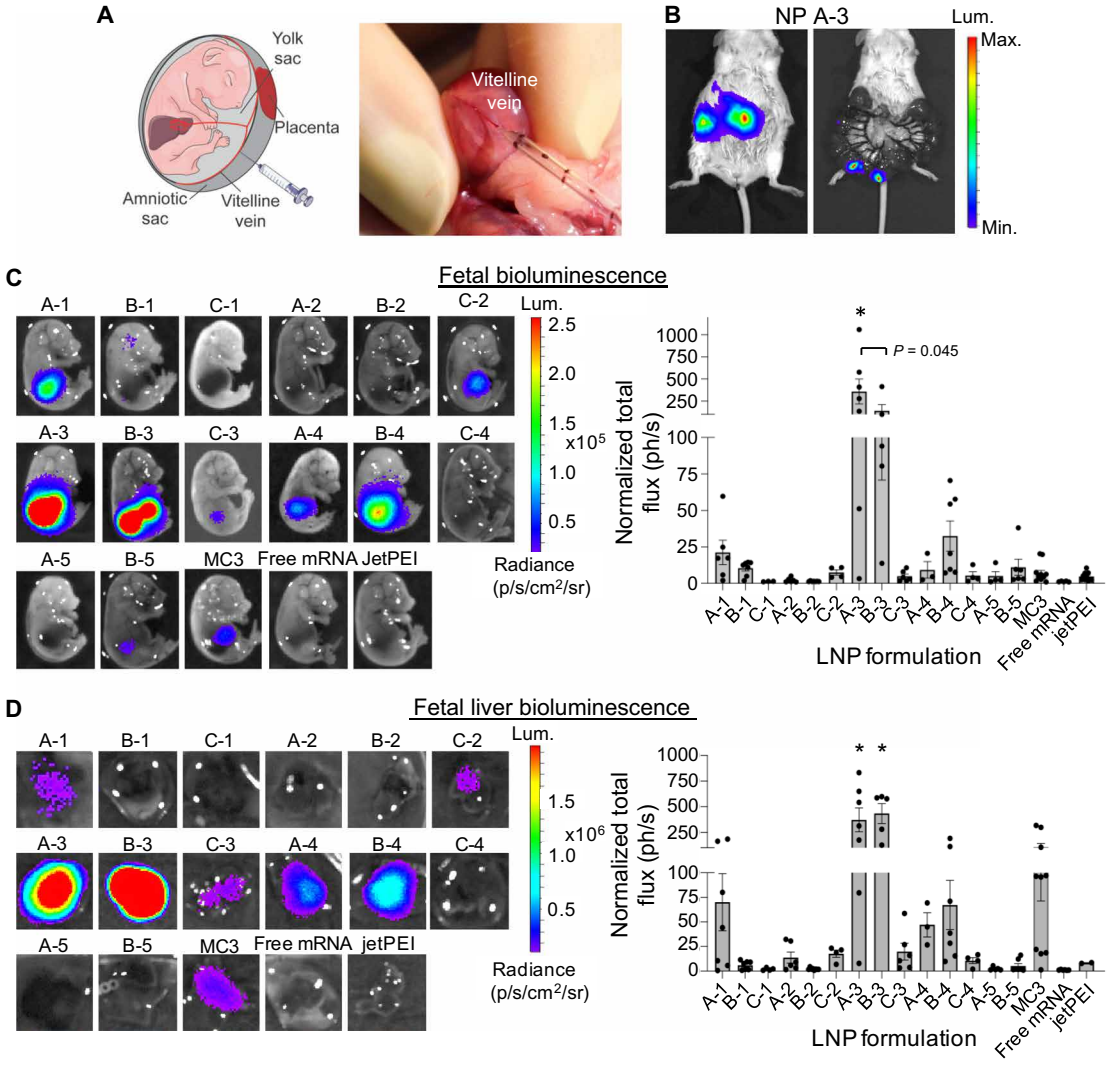

Fig. 3. LNP-mediated mRNA delivery to fetuses. (**A**) Schematic (left) and photograph (right) showing the vitelline vein injection in a mouse fetus. Photo credit: Andrew Cheng, The Children's Hospital of Philadelphia. (**B**) IVIS imaging showing luciferase expression in a representative dam (left) and within the exposed uterine horn (right). (**C**) IVIS images (left) and quantification (right) of luciferase signal in fetuses following surgical removal from dams. (**D**) IVIS images (left) and quantification (right) of luciferase signal from livers of fetuses injected with LNPs. Each fetus was injected via the vitelline vein, extracted, and imaged by IVIS 4 hours after injection. Quantifications are the normalized total flux calculated by dividing the luminescence from the area of interest by the background from each individual image. The normalized total flux was averaged across injected fetuses. *$P < 0.001$ by one-way analysis of variance (ANOVA) with post hoc Tukey-Kramer compared to all other treatment groups, unless indicated otherwise, and outliers were detected using Grubbs' test and removed from analysis; minimum $n = 3$ per treatment group; error bars represent SEM.

or other fetuses in the uterine horn. After imaging the dams, experimental and control fetuses were surgically removed to allow for more precise comparison of the efficiency of mRNA delivery between different LNPs (Fig. 3C and fig. S2). The fetuses were imaged individually by IVIS (Fig. 3C), and the normalized luminescent signal was subsequently quantified. For each image, a rectangular region of interest (ROI) was placed over the fetus, and a second ROI of the same size was placed over an area of the image off of the fetus as background. The same-sized ROIs were used in every image for each quantified tissue, and ROIs were consistently placed over the same area of each fetus or tissue (fig. S3). The reported normalized luminescence represents the total flux from the ROI placed over the fetus divided by the total flux from background ROI. By quantifying the luminescent data in this manner, we were able to account for the minor differences in background luminescence between fetuses treated on different days. Some LNP formulations yielded greater mRNA delivery compared to others, indicating that the ionizable lipid within the LNPs strongly dictates their ability to deliver mRNA to fetuses. Specifically, LNPs A-1, A-3, B-3, and B-4 yielded the strongest luciferase signal (Fig. 3, C and D, and fig. S2), and no fetuses injected with free mRNA yielded detectable luciferase signal at the imaging parameters used in these experiments, indicating the need for LNPs for efficient mRNA delivery.

LNPs outperform benchmark lipid and polymeric delivery systems DLin-MC3-DMA and jetPEI

We next aimed to compare our LNP platforms against the widely studied in vivo nucleic acid delivery systems, DLin-MC3-DMA

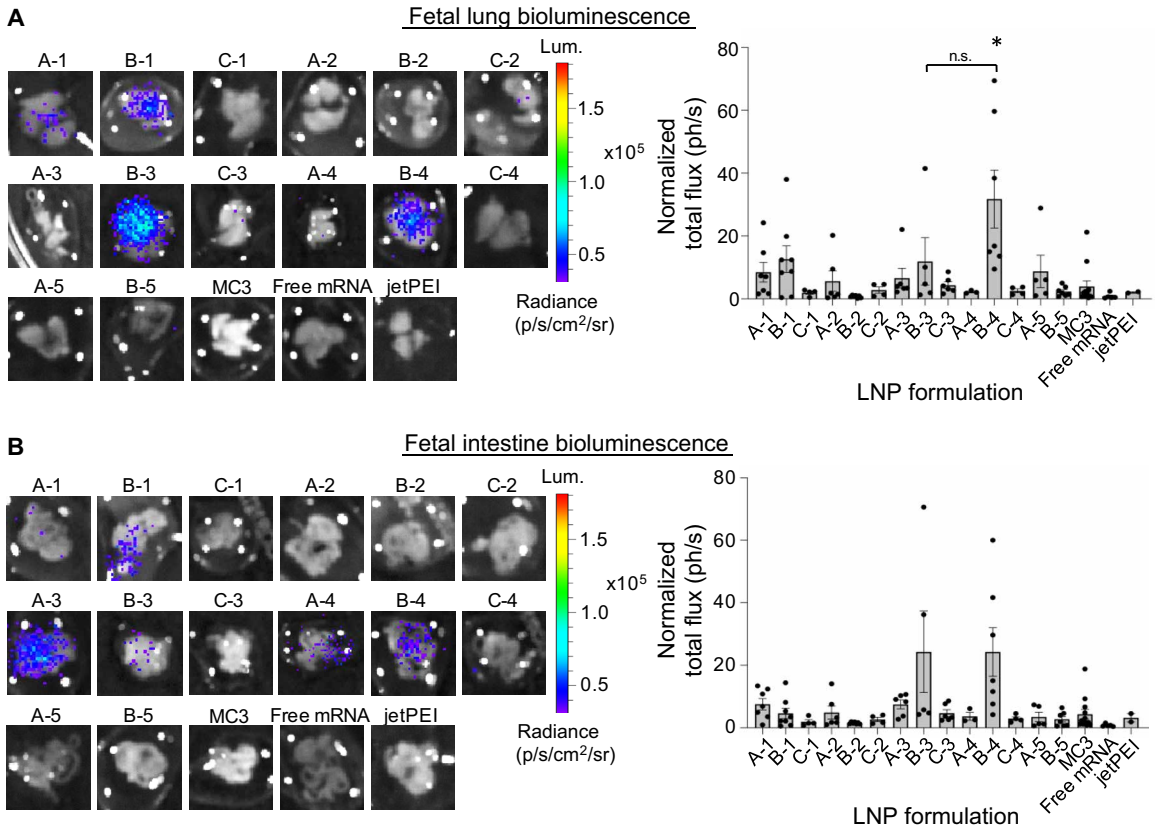

Fig. 4. LNP-mediated mRNA delivery to fetal intestines and lungs. (**A**) IVIS images (left) and quantification (right) of luciferase signal in the lungs. n.s., not significant. (**B**) IVIS images (left) and quantification (right) of luciferase signal in the intestines. Normalized total flux was averaged across injected fetuses. *$P < 0.05$ by one-way ANOVA with post hoc Tukey-Kramer compared to all other treatment groups, unless indicated otherwise; minimum $n = 3$ fetuses per treatment group; error bars represent SEM.

(MC3) and jetPEI, for in utero delivery (*44*–*47*). MC3 and jetPEI have been evaluated for nucleic acid delivery in clinical trials, making their comparison to our LNPs a critical benchmark for in vivo mRNA delivery (*45*, *48*, *49*). Furthermore, the MC3 lipid was recently approved by the U.S. Food and Drug Administration (FDA) for clinical use for small interfering RNA (siRNA) delivery to treat polyneuropathy in patients with hereditary transthyretin-mediated amyloidosis (*45*–*47*). Fetuses injected with jetPEI (jetPEI.luc) complexes yielded only a modest increase in luminescence compared to free luciferase mRNA 4 hours after injection (Fig. 3C and fig. S2). Several of our LNP formulations were more efficient for mRNA delivery compared to jetPEI.luc, and our top-performing LNP A-3.luc demonstrated a 75-fold increase in luminescence over jetPEI.luc. As a second commercially available comparison, we incorporated the ionizable lipid MC3 into LNPs (MC3.luc) to directly compare in utero mRNA delivery between our ionizable lipids and this gold standard lipid. MC3.luc delivered mRNA to fetal livers, although not to the same extent as our top-performing LNPs A-3.luc and B-4.luc. Quantification of normalized total flux in the fetal livers revealed a 3.5-fold and 4-fold decrease in luminescence compared to LNPs A-3 or B-3, respectively. Collectively, these results indicate that LNPs developed in this study induced greater in utero protein expression in fetal livers than benchmark lipid and polymeric delivery systems currently used for nucleic acid delivery.

Intravascular LNP injection primarily results in mRNA delivery to fetal livers

Imaging of the pregnant dams and individual fetuses demonstrated the ability of our LNP.luc formulations to selectively deliver mRNA to the fetus while avoiding crossover to the dam. We next sought to evaluate which, if any, organs experienced preferential accumulation of any of the LNP formulations. The liver, lungs, brain, kidney, heart, and intestines from injected fetuses were isolated and analyzed by IVIS 4 hours after treatment. The brightest signal was detected in livers from fetuses injected with LNPs (Fig. 3D and fig. S2). This is likely due to a first-pass effect, as the vitelline vein drains directly into the portal circulation and forms the hepatic sinusoids (*43*). The normalized total luminescent flux from fetal livers injected with the various LNP formulations correlated well with the normalized total luminescent flux from the whole fetus (Fig. 3C compared to Fig. 3D), indicating that the majority of the signal noted on whole fetal analysis resulted from LNP-mediated mRNA delivery to the fetal liver.

Analyses of kidneys and hearts following delivery of any of the LNP.luc formulations demonstrated minimal detected luminescent signal at the scale range used in these studies (fig. S2). A low level of luminescent signal was noted in the brains of fetuses injected with a few LNPs, such as B-3.luc (fig. S2). In addition to demonstrating high levels of liver bioluminescence, fetuses injected with LNPs A-3.luc, B-3.luc, and B-4.luc had luminescent signal in the lungs and

intestines (Fig. 4 and fig. S2). Because both of these LNPs consisted of ionizable lipids with the C12 or C14 epoxide-terminated alkyl tails, we anticipate that the ability of these LNPs to deliver mRNA to the lung and intestines is due to the combination of similar polyamine core structures (polyamine core 3 is a branched form of polyamine core 4) in each of these formulations with these alkyl tails. However, further testing is needed to evaluate the specific mechanism by which these formulations can surpass the liver to reach the lungs and intestines. Last, LNP MC3.luc delivered mRNA to the liver, with minimal delivery to lungs and intestines, and luciferase expression induced by jetPEI.luc was not observed in any organs at the imaging scales used here (Fig. 3D and fig. S2).

Fully saturated ionizable lipids induce maximal mRNA delivery

Because the polyamine-lipid synthesis contained more than one level of alkyl chain substitutions (fig. S4), we evaluated the mRNA delivery capabilities of only the fully saturated core. To do this, we purified the fully saturated polyamine-lipid core by flash chromatography and used the purified material, rather than the crude material, to prepare the A-3 and B-4 LNP formulations (termed pA-3.luc and pB-4.luc, respectively). The purified products were confirmed to be fully saturated with the lipid epoxides by liquid chromatography–mass spectrometry (LC-MS) (fig. S4).

The efficiency of luciferase mRNA delivery by LNPs pA-3.luc and pB-4.luc was compared to that achieved via delivery by LNPs A-3.luc and B-4.luc (prepared with crude material) to ensure that the fully saturated ionizable lipids were primarily responsible for mRNA delivery. Injected fetuses were imaged by IVIS after 4 and 24 hours after injection (fig. S5). There was only a modest reduction in luciferase signal in the whole fetus and isolated livers following injection with the purified LNPs. These findings are consistent with previous studies and believed to be due to the polyamine cores in the crude mixture having a broad range of alkyl chain substitutions yielding higher mRNA delivery (*50*). However, given their clinical relevance and only a modest difference in mRNA delivery, LNPs pA-3 and pB-4 were used in the subsequent studies to induce hepatic protein expression. As expected, the luciferase signal was transient; the brightest signal was detected at 4 hours after injection with decreasing levels at 24 hours after injection. Moving forward, there is potential to study repeated doses of LNPs, additional modifications to the mRNA cargo, or more permanent gene therapies, for prolonged therapeutic efficacy (fig. S5).

LNPs enable delivery of GFP mRNA and EPO mRNA as a model for protein replacement therapy

We next sought to demonstrate that our LNPs are robust and have the ability to deliver multiple types of mRNAs to fetuses. Green fluorescent protein (GFP) mRNA, which is detectable by fluorescence analysis techniques, was encapsulated within LNPs A-3 and B-4 (A.3.GFP and B-4.GFP) and delivered via the vitelline vein to E16 fetuses, and GFP expression was assessed 24 hours after injection via fluorescent stereomicroscopy and flow cytometry. Similar to luciferase expression following injection of LNPs A-3.luc and B-4.luc, GFP was expressed in the fetal livers (Fig. 5, A and B). Furthermore, treatment with LNP A-3.GFP resulted in stronger GFP fluorescence in the liver at 24 hours after injection compared to treatment with LNP B-4.GFP as demonstrated by both fluorescence imaging and flow cytometry (Fig. 5, A and B). For flow cytometry, fetal livers were processed into a single-cell suspension and stained for CD45, which is a marker for hematopoietic cells. The $CD45^-$ population was used to determine the population of GFP-expressing cells from the liver tissue, which revealed that LNPs A-3 and B-4 yielded 1.1 and 0.17% GFP^+ cells in the liver, respectively. The GFP data are consistent with our previous work on adeno-associated virus to deliver GFP mRNA to fetal livers (*16*). These results agree with our luciferase data suggesting that LNP A-3 yields higher mRNA delivery to fetal livers compared to LNP B-4 or PBS and that the results of the LNP.luc screen are translatable to the prenatal delivery of other mRNAs.

Last, to demonstrate the therapeutic potential of our LNPs, we assessed prenatal delivery of human EPO mRNA in LNP pA-3 (LNP pA-3.EPO) and LNP pB-4 (LNP pB-4.EPO). Successful liver delivery with LNPs pA-3.EPO or pB-4.EPO would result in hepatic production of EPO protein, which is then secreted into the circulation. This model is relevant to a number of enzyme deficiency disorders, such as the lysosomal storage diseases, which cause irreversible damage before birth and for which hepatic production and secretion of the deficient enzyme is being pursued as a viable therapy (*3*). LNP pA-3.EPO and pB-4.EPO were injected through the vitelline vein into E16 fetuses at two different doses (5 μl = 190 ng EPO mRNA or 20 μl = 760 ng EPO mRNA), and fetal livers were assessed by enzyme-linked immunosorbent assays (ELISAs) for human EPO protein at 4 and 24 hours after injection (Fig. 5C). Mouse fetuses injected with PBS as a control revealed that human EPO is not present or detected in the fetal livers at baseline (Fig. 5C). Therefore, the presence of EPO indicates successful LNP and mRNA delivery to fetal livers. There was a clear dose-dependent response in EPO production following treatment with LNPs at both time points. This is exemplified by the fivefold higher EPO expression at 4 hours in fetuses injected with the higher volume of pA-3. EPO compared with those injected with the lower volume (Fig. 5C). Furthermore, fetal livers collected 24 hours after injection had lower EPO content compared to those collected 4 hours after injection, similar to our results with luciferase mRNA delivery. Last, LNP pA-3.EPO yielded twofold higher EPO content than LNP B-4.EPO 4 hours after injection. These results strongly agree with our luciferase and GFP expression data, confirming that these LNP platforms are robust and have the ability to deliver several types of mRNA, including those that model protein replacement therapies to treat prenatal disease.

LNPs are safe for nucleic acid delivery to fetuses and do not induce fetal loss

Survival and toxicity were assessed at E19 following LNP injection at E16 to remove the variables of poor parenting and pup death related to the natural birthing process. As such, injected fetuses were delivered by cesarean section and assessed for gross appearance, presence of spontaneous movements, and visible precordial palpations (heartbeat) to assess for survival at E19 (Fig. 6A and fig. S6A). Balb/c fetuses injected with either LNP pA-3.luc or pB-4.luc had >90% survival, which was comparable to control fetuses injected with PBS. Alternatively, fetuses injected with LNP MC3.luc had a survival rate of 72.4%. These results suggest that survival from in utero delivery of our LNPs (LNP pA-3.luc and pB-4.luc) is no different from that associated with the procedural related toxicity in the mouse model. Furthermore, our results suggest that LNP MC3. luc may be more toxic to fetuses compared to our LNPs, although the difference in survival between each treatment group was not

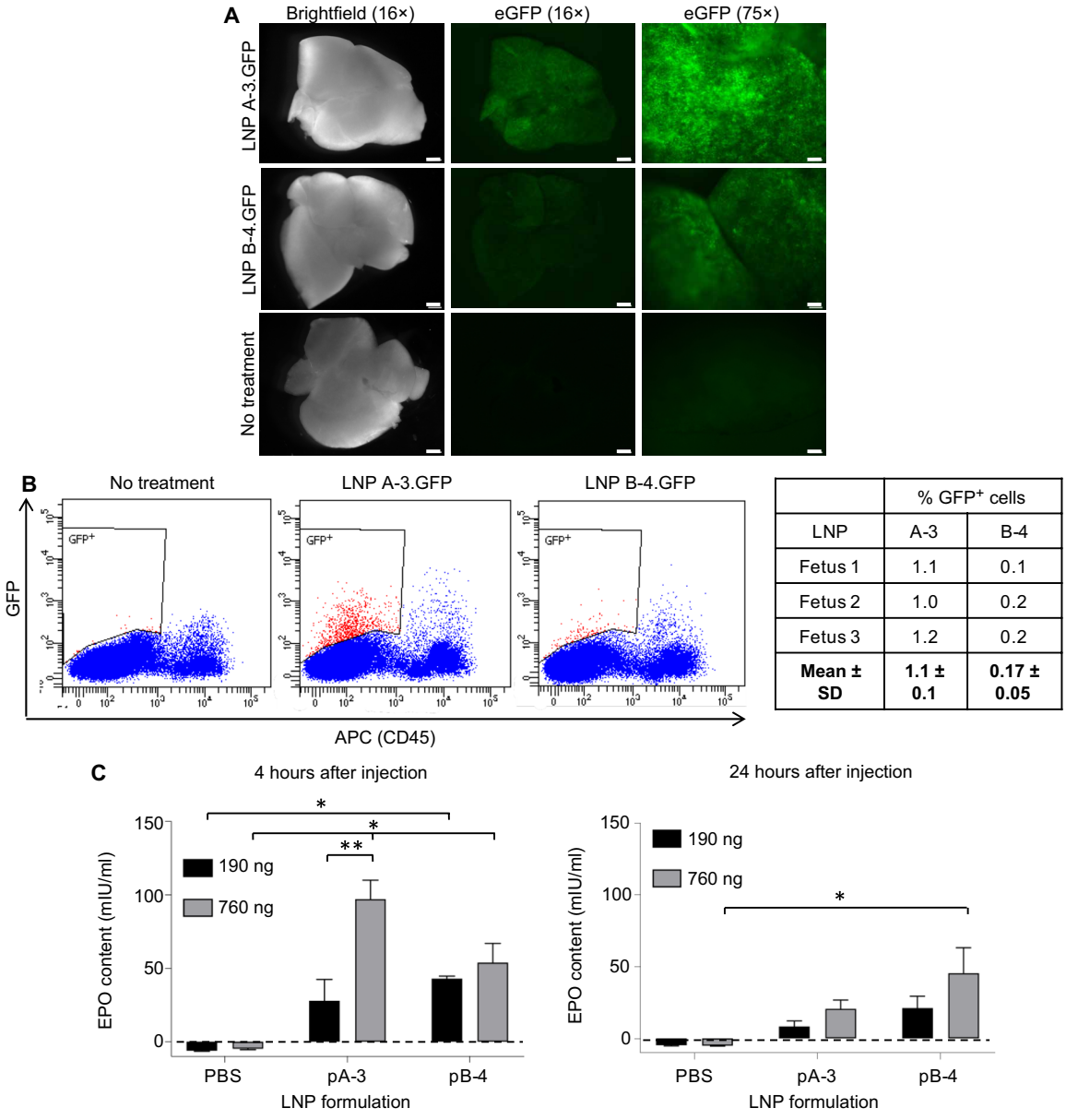

	% GFP⁺ cells	
LNP	A-3	B-4
Fetus 1	1.1	0.1
Fetus 2	1.0	0.2
Fetus 3	1.2	0.2
Mean ± SD	**1.1 ± 0.1**	**0.17 ± 0.05**

Fig. 5. LNPs deliver GFP mRNA and EPO mRNA in utero. (**A**) GFP expression in fetal livers 24 hours after injection with LNPs A-3.GFP or B-4.GFP, or PBS. Scale bars, 150 μm (75×) and 750 μm (16×). eGFP, enhanced GFP. (**B**) The same fetal livers in (A) were processed into single-cell suspensions and analyzed using flow cytometry to record the percentage of $CD45^-$ and GFP^+ cells. Dot plots show one liver sample per treatment group to demonstrate the gating and quantification. (**C**) EPO content in fetal livers (left) at 4 hours (left) or 24 hours (right) after injection of LNPs pA-3.EPO or pB-4.EPO, or PBS. EPO concentrations were averaged across three fetuses per treatment group and analyzed by two-way ANOVA comparing mean EPO concentration among treatment groups; $^*P < 0.02$ and $^{**}P < 0.001$; error bars represent SEM.

statistically significant. We also evaluated survival following LNP injection in C57BL/6 fetuses to directly compare LNP toxicity in different strains of mice. All C57BL/6 treatment groups had 100% survival, indicating that prenatal delivery of our LNPs does not result in loss of viability in C57BL/6 mice, and there is minimal difference in survival between C57BL/6 and Balb/c strains (fig. S6A).

LNP injections result in minimal fetal immunotoxicity or liver damage

Given the high efficiency of liver accumulation of our LNPs, we next sought to determine whether prenatal LNP delivery resulted in liver toxicity or activation of an inflammatory response in the fetus or dam. First, we sought to demonstrate that the mRNA used in this study is not independently immunogenic. We transfected human dendritic cells with luciferase mRNA or EPO mRNA and evaluated interferon-α (IFN-α) expression levels in the culture media after 24 hours. Following treatment, there was no increase in IFN-α levels, indicating that the mRNA itself is not immunogenic (fig. S7).

Fetal liver toxicity following LNP injection was assessed by quantifying the liver enzymes alanine aminotransferase (ALT) and aspartate aminotransferase (AST) from fetal liver tissue at E19. There was a minor increase in AST levels from all LNP- and PBS-injected

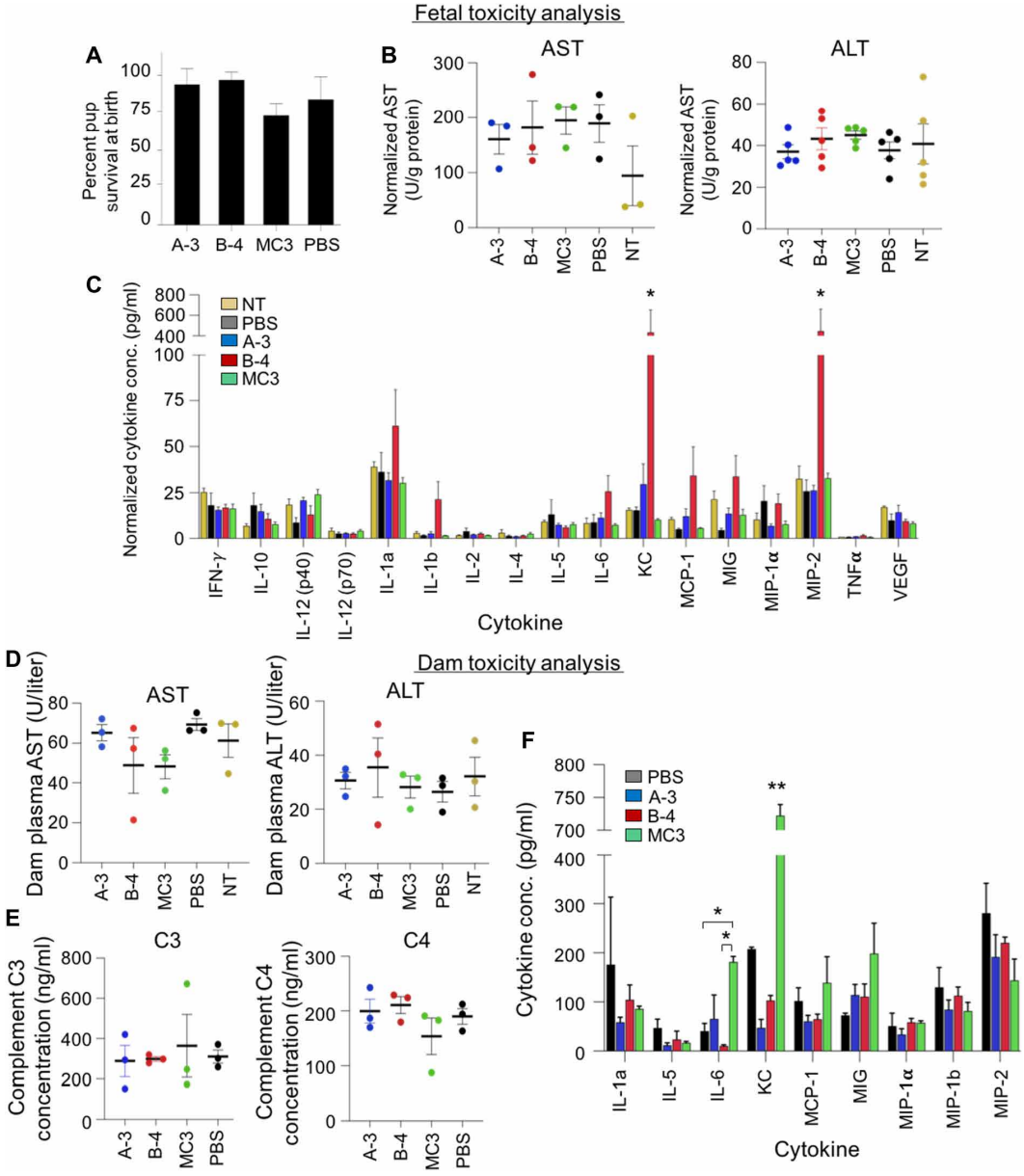

Fig. 6. Evaluation of fetal survival and toxicity following LNP injections. (**A**) Percent survival of fetuses injected at E16 and surgically delivered at E19. Survival was determined immediately following extraction. Error bars represent SD from three dams following injection to every fetus in each dam. (**B**) Liver enzyme analysis from fetal liver tissue collected at E19 following injection at E16. Measured AST or ALT units were normalized by dividing by protein concentration from fetal liver tissue. (**C**) Cytokine analysis from fetal livers collected immediately following surgical delivery at E19. *$P < 0.0001$ by two-way ANOVA compared to each treatment group for each cytokine; $n = 5$ fetuses per treatment group. (**D**) Liver enzyme analysis, (**E**) complement system activation, and (**F**) cytokine analysis from plasma collected from dams at E19 before surgical delivery of the injected fetuses. The following cytokines were out of range of the instrument and is therefore not shown: IFN-γ, IL-10, IL-12 (p40), IL-12 (p70), IL-1b, IL-2, IL-4, tumor necrosis factor–α (TNFα), and vascular endothelial growth factor (VEGF); $n = 3$ dams per treatment group. *$P < 0.02$ and **$P < 0.0001$ by two-way ANOVA compared to each treatment group for each cytokine; $n = 3$ dams per treatment group. Error bars in (B) to (F) represent SEM with outliers detected by Grubbs' test and removed from analysis.

mice compared to untreated controls that was not statistically significant. However, AST levels following injection with our LNPs pA-3.luc and pB-4.luc were comparable to mice treated with either MC.3.luc or PBS. This indicates that the injection procedure itself may affect AST levels. There were no significant changes in ALT or AST levels from fetal livers treated with our LNPs or controls, indicating that our LNPs enable nucleic acid delivery to fetal livers without inducing enzyme release–associated toxicity at the time points evaluated here (Fig. 6B).

We next evaluated the induction of an inflammatory response to LNPs pA-3.luc and pB-4.luc, and MC3.luc to further elucidate their safety for fetal therapy. We assessed cytokine production from E19 livers of Balb/c fetuses that had been injected with LNPs pA-3.luc and pB-4.luc, MC3.luc, or PBS (Fig. 6C). Most cytokine levels were not significantly

different in LNP-treated fetuses compared to untreated or PBS-treated control fetuses. No cytokines were elevated in response to LNP pA-3.luc, our top-performing LNP for mRNA delivery. Two chemokines, KC (keratinocytes-derived chemokine) (also termed IL8/CXCL1) and macrophage inflammatory protein 2 (MIP-2) (also termed CXCL2), were elevated in fetal livers in response to LNP pB-4.luc. These two chemokines are potent neutrophil attractants and play a role in inflammation, wound healing, angiogenesis, and other biological processes (*51*). To evaluate any mouse strain–specific cytokine response to the LNPs, we conducted a similar analysis on E19 fetal livers harvested from C57BL/6 mice injected with LNPs pA-3.luc, pB-4.luc, MC3.luc, or PBS. This analysis did not reveal an increase in KC and MIP-2 levels similar to that found in Balb/c mice (fig. S6B). Rather, treatment with our LNPs in C57BL/6 mice resulted in decreased MIP-2 expression and increased MIG (monokine induced by gamma) and vascular endothelial growth factor (VEGF) levels compared to PBS injections (fig. S6B). These differences between Balb/c and C57BL/6 mice may be partly due to the fact that they develop different T cell–mediated immune responses (*52*).

Lack of maternal toxicity following in utero LNP delivery

Any fetal intervention involves two patients, the fetus and the mother, that could be potentially affected by the treatment (*53*). Thus, we also evaluated the toxicity of prenatal LNP delivery on the pregnant dams. No maternal deaths (both Balb/c and C57BL/6 dams) were noted following in utero LNP delivery throughout all of the experiments. There were no differences in ALT and AST levels between Balb/c dams whose fetuses were injected with LNPs pA-3.luc, pB-4.luc, MC3.luc, or PBS (Fig. 6D), suggesting that in utero LNP delivery did not result in maternal liver toxicity. Maternal Balb/c plasma was also assessed for C3 and C4 levels to assess complement activation in the mothers of fetuses undergoing in utero LNP or PBS injection, and no significant differences were noted between experimental and control mice (Fig. 6E). Last, analysis of cytokine levels from plasma collected from Balb/c dams at E19 revealed few significant changes between those injected with LNPs or PBS, and the majority of cytokines tested were below the assay's detection level (Fig. 6F). Of note, KC and interleukin-6 (IL-6) were significantly up-regulated in serum of dams with fetuses injected with LNP MC3.luc compared to other treatment groups (Fig. 6F). These results demonstrate that our LNPs do not induce liver damage, an inflammatory response, or activation of the complement system in the dams of injected fetuses.

DISCUSSION

Because of recent expansions in carrier screening, as well as advances in chromosomal microarray analysis and whole-exome sequencing, a large number of clinically relevant monogenic diseases can be diagnosed prenatally (*54*). Among these are hemoglobinopathies (α- and β-thalassemia and sickle cell anemia), enzyme deficiencies (urea cycle disorders and glycogen storage diseases), and protein deficiencies (cystic fibrosis and α-1 antitrypsin) (*10*–*14*). Though there are more than 100 postnatal enzyme and protein replacement therapies, these are limited by cost, adverse effects including hypersensitivity and immune response, limitations in reaching the desired organs, and an inability to reverse or rescue already damaged tissue (*55*, *56*). Gene therapy, specifically mRNA therapeutics, has recently gained traction as a method of inducing protein or enzyme expression in vivo, with multiple studies demonstrating a longer-term expression of the substrates compared to conventional replacement therapy (*57*, *58*). However, research involving prenatal mRNA delivery is in a nascent stage of development.

Fetal gene therapy has multiple advantages compared to postnatal therapy including a larger population of progenitor cells that can be treated and expanded, reduced immunogenicity due to the immature fetal immune system, and, most importantly, the ability to deliver therapeutics early or before the onset of phenotypic abnormalities (*6*, *7*, *15*). Furthermore, prenatal therapy can enable maximization of injected dosage per weight to reduce therapy and manufacturing costs, as a human fetus at 16 weeks' gestation weighs approximately 100 g, compared to 4000 g at birth. This translates to a 40-fold lower required dosage compared to postnatal therapy when administered at 16 weeks' gestation. Now, prenatal interventions are diagnostic or limited to the treatment of specific diseases such as twin-twin transfusion syndrome (*59*), congenital diaphragmatic hernia (*60*), and myelomeningocele (*61*). Furthermore, in utero hematopoietic stem cell transplantation has recently entered clinical trials for α-thalassemia major (NCT02986698), demonstrating precedence and need for advanced prenatal therapeutics. Thus, LNP-mediated delivery of nucleic acids has the potential to benefit the numerous fetal diseases that can be treated following prenatal diagnosis.

Toward this goal, we developed and evaluated a library of LNP formulations for fetal nucleic acid delivery. Developing nanomaterials specifically for a particular application, such as fetal delivery, is critical because small changes in LNP chemistry, such as using different ionizable lipids, can greatly affect their ability to accumulate within the desired tissues and deliver the encapsulated mRNA (*14*). There have been minimal studies conducted that evaluate NP delivery platforms for fetuses, although LNPs have been extensively studied in adult mice (*34*–*36*). Previous work for fetal nucleic acid delivery has focused on PLGA NPs to deliver peptide nucleic acids, which are triplex-forming DNA analogs that induce endogenous DNA repair (*15*, *62*). This critical prior study used PLGA NPs to successfully treat a mouse model of β-thalassemia. In this study, our focus revolved around the investigation of ionizable lipid structures within LNPs specifically for nucleic acid delivery to fetuses, and future work will evaluate our top ionizable lipid structures within LNPs to treat specific disease models.

Lipid-based materials, such as those developed here, enable a substantial amount of compositional flexibility. For example, the polyamine cores are easily interchangeable with epoxides of different lengths to develop diverse libraries of materials (Fig. 2). Furthermore, the excipients used to make LNPs, as well as the molar ratios, enable additional design flexibility to LNP composition, all of which affect delivery and transfection. For example, 1,2-distearoyl-*sn*-glycero-3-phosphocholine (DSPC), rather than DOPE, has also been used as the phospholipid excipient in LNP formulations for mRNA or siRNA delivery to adult mice (*35*, *40*, *42*). In this work, we designed ionizable lipids to evaluate how polyamine-lipid core materials affect prenatal delivery, but future work in LNP development for fetal diseases may explore how various excipient compositions can be tailored for specific nucleic acid cargos such as siRNA or gene editing technologies.

Prior studies using LNP delivery systems have shown high safety profiles and transfection efficiency in livers of adult mice, demonstrating

biocompatibility and therapeutic applicability, particularly compared to cationic lipid nanocarriers (*34*, *35*, *44*). Because of these prior studies, we anticipated that ionizable LNPs could be developed for nucleic acid delivery to fetuses to enable prenatal therapy without the use of viral delivery mechanisms (*11*). Furthermore, we anticipated that our LNPs would yield better safety profiles, leading to lower toxicity compared to cationic lipid and polymer carriers such as DLin-MC3-DMA and jetPEI, which have been used in clinical trials to treat adult disease (*44*, *48*). The library of LNPs developed and tested here provides several ionizable lipid materials that can be used for delivery to fetal livers, lungs, and intestines. Hepatic delivery was anticipated following the route of administration via the vitelline vein, as this vein directly leads to the liver sinusoids (*43*). We found several polyamines, structures 3 and 4, that yielded the highest transfection efficiency when complexed into LNPs (Figs. 2 to 4). These two high-performing polyamines have the most structural similarities out of the five distinct structures tested, as polyamine 3 is a branched version of polyamine 4 with the same number of amines and oxygen groups. From our results, we can conclude that the chemical composition of these cores is critical for fetal delivery of mRNA, and the branched polyamine yields stronger mRNA delivery compared to the linear version.

A notable finding was that our lead ionizable LNPs outperformed both jetPEI and LNPs composed of the DLin-MC3-DMA lipid in terms of mRNA delivery and safety. Our top ionizable LNP yielded a 45- and 3.5-fold increase of normalized luminescence in the liver compared to jetPEI.luc complexes and LNP MC3.luc, respectively. Luminescence in fetuses injected with jetPEI.luc was both qualitatively and quantitatively similar to our lowest-performing LNPs. The high survival rates from injections with our LNPs (>90%) are comparable to ours and others' previous work with vitelline vein injections (*5*, *63*, *64*). The reduction in survival (although not statistically significant) of LNP MC3.luc compared to our LNPs may indicate increased toxicity of MC3.luc. Because the survival rates following injection with LNPs A-3.luc, B-4.luc, or PBS are similar, this loss in viability from MC3.luc can likely be attributed to toxicity of the LNP itself or to the technical challenges of prenatal intravascular injections in the mouse model. The ability of our top LNPs to outperform the commercially available and FDA-approved DLin-MC3-DMA lipid for mRNA delivery to fetuses is a key aspect of the innovation in this work.

Furthermore, we demonstrated that our LNPs can deliver a range of mRNAs, including GFP and EPO mRNA. We chose to deliver EPO mRNA prenatally in our top LNP formulations because it is commercially available, it is extensively tested, and the protein produced from the delivered mRNA is easily quantified through commercially available assays. Furthermore, EPO represents a potentially therapeutic and disease-relevant mRNA. For example, fetal anemia is a serious condition that can arise from multiple etiologies including alloimmunization, infection, genetic disorders such as lysosomal storage diseases and inherited anemias, and other structural abnormalities (fetal/placental tumors, vascular malformations, etc.) (*65*, *66*). In its most severe form, repeated fetal blood transfusions are required to prevent in utero demise or neonatal morbidity and mortality. LNP delivery of EPO mRNA to stimulate endogenous red blood cell (RBC) production may provide an alternative treatment to multiple invasive fetal blood transfusions for select fetal anemias, including those of infectious etiology. Toward this goal, exogenous EPO protein delivery has been shown to treat fetal anemia resulting in either the elimination or significant reduction in the need for blood transfusions in a sheep model of extrauterine support of fetal/premature lambs (*67*). The levels of EPO protein production seen in the fetal liver in our studies 24 hours after LNP-EPO mRNA delivery were ~65% (LNP A-3) to 145% (LNP B-4) of the levels in the serum of lambs before the onset of anemia and ~515% (LNP A-3) to 1130% (LNP B-4) of the levels in the serum of lambs at the time of anemia, suggesting that therapeutic levels of EPO production could be provided by LNP-EPO mRNA delivery.

Furthermore, by delivering mRNA, one can capitalize on the natural posttranslational protein modifications that occur, and the persistence of the therapeutic effect may be enhanced to minimize the need for repeated fetal interventions (i.e., repeat transfusions or protein administration). Last, EPO mRNA also serves as a proof of concept for the potential of LNP-mediated mRNA delivery for other congenital diseases. For example, MPS VII (Mucopolysaccharidosis type VII), or Sly syndrome, results from a deficiency of β-glucuronidase and is a leading genetic cause of fetal hydrops and fetal demise. When patients with MPS VII do survive to birth, they often have multiorgan dysfunction including cardiac, pulmonary, skeletal, and neurodevelopmental abnormalities. A recent study demonstrated the potential to rescue the disease phenotype in the mouse model of MPS VII via in utero enzyme replacement therapy with recombinant human β-glucuronidase (rhGUS). In utero enzyme replacement was shown to have advantages over postnatal enzyme replacement (*68*). In utero LNP delivery of the *BGUS* mRNA may serve an alternative approach that capitalizes on the advantages of endogenous protein production detailed above.

The high survival rates and, in general, similar cytokine production profiles, liver enzyme, and complement levels between experimental and control animals suggest that there is minimal maternal or fetal toxicity associated with in utero LNP injections and mRNA delivery. However, our data revealed that LNP B-4.luc may initiate an immune response in Balb/c fetuses as indicated by increased KC and MIP-2 levels. However, the elevation in KC and MIP-2 production was strain specific and not seen in C57BL/6 fetuses. KC and MIP-2 are cytokines activated in response to injury, stress, and inflammation (*69*). One potential explanation for the increase in KC and MIP-2 in LNP B-4.luc–injected Balb/c fetuses is the persistence of this LNP in the fetal tissue longer than other LNP formulations. This hypothesis and a more robust analysis of the effect of different ionizable lipid structures and mouse strains on the inflammatory response of LNP-injected fetuses are the subject of future studies.

We found several LNPs that were able to deliver mRNA to the lungs and intestines at the doses injected in these experiments, albeit at low transfection efficiencies, in addition to the fetal liver. We expect that this trait is due to the chemical structures of LNPs A-3.luc, B-3.luc, and B-4.luc as these contained the C12 or C14 epoxide-terminated alkyl tails with the two top-performing polyamines 3 or 4. The LNPs prepared with the C16 epoxides and these polyamine cores yielded minimal luciferase signal in any organs aside from the liver, demonstrating that the epoxide size may be a critical component for delivery to other fetal organs. These data demonstrate that the polyamine-lipid core structure and the lipid epoxide length are important for enabling mRNA delivery to these organs, although the level of mRNA delivery seen here may not yield therapeutic benefits in a disease model. Because of efficient liver delivery and low overall level of delivery to other tissues, we only conducted

toxicity experiments on the liver. Moving forward, these LNPs will be further optimized to enable increased nucleic acid delivery to treat fetal diseases that originate in the lungs and intestines, at which time extensive toxicity analyses on the tissues of interest will be critical. However, it is important to note that other ionizable LNPs have been evaluated for safety in adult mice, in nonhuman primates, and in clinical trials in humans, which have demonstrated low toxicity overall (*70*–*72*). Therefore, it is reasonable to anticipate that future studies will yield high safety to other tissues, as well as the liver, which was the tissue of interest in the present study.

The experiments conducted here used a single in utero injection due to the short murine gestation of 20 days. Our overarching goal was to screen LNP formulations prepared from ionizable lipid materials, so we chose shorter end points that covered the course of gestation postinjection (at E16) to birth to assess luciferase activity as well as pup survival and toxicity associated with our LNPs. When translated to large animal models or humans with longer gestations, multiple injections would be feasible to increase the amount and/or duration of expression of delivered nucleic acids and their resultant therapeutic efficacy. In these larger models and humans, injections would be performed without the need for a laparotomy but, instead, via an ultrasound-guided approach as is currently performed for amniocentesis or a cord blood transfusion, both of which are relatively noninvasive and regularly performed in the clinic. For example, fetuses with hemoglobin Bart's hydrops fetalis associated with α-thalassemia have safely undergone multiple ultrasound-guided cord blood transfusions before birth (*8*, *73*). Thus, future studies in large animal models should determine the efficacy and toxicity of repeat dosing. Furthermore, treatment protocols after birth would need to be considered given the transient nature of the LNP-mRNA therapy. These postnatal treatments would be highly disease specific and dependent on the mRNA being prenatally delivered. In utero delivery of LNP-mRNAs to replace a deficient protein or enhance endogenous protein expression may be adequate without additional postnatal treatments for disease states in which the offending agent is no longer present after birth, as is the case with some fetal anemias. Alternatively, if LNPs are used to deliver mRNA to replace a deficient enzyme associated with a genetic disease, then continued postnatal treatments would be necessary unless LNPs are used to correct the underlying genetic mutation.

In conclusion, we have developed and screened LNP platforms for nucleic acid delivery that could ultimately be used to treat monogenic fetal diseases that do not currently have sufficient therapeutic options in the prenatal setting. These LNPs yielded higher hepatic delivery and transfection efficiency with advantageous safety profiles compared to the commercially available delivery agents DLin-MC3-DMA and jetPEI, which are considered benchmarks for in vivo nucleic acid delivery. Although much work has been done evaluating the therapeutic potential of LNPs after birth, little work, to our knowledge, has been done assessing the ability to use ionizable LNPs before birth. Moving forward, we will use this platform to deliver disease-specific, therapeutic nucleic acids in animal models of human diseases as a therapeutic approach for congenital disorders.

MATERIALS AND METHODS

Polyamine-lipid synthesis and purification

The ionizable lipid cores were prepared via Michael addition chemistry as previously described (*34*). Briefly, the polyamine cores (purchased from Enamine Inc., Monmouth Junction, NJ) were combined with excess moles of lipid epoxide needed to saturate the amines in 4-ml amber vials with a magnetic stir bar. The lipid epoxides used in this study were epoxydodecane (C12), epoxytetradecane (C14), or epoxyhexadecane (C16) (Sigma-Aldrich, St. Louis, MO). The vial was sealed and the reaction was mixed for 2 days at 80°C. The crude reaction mixture was dried using a Rotovap R-300 (Buchi, New Castle, DE), and the crude reactions were used for screening the library with luciferase mRNA. The A-3 and B-4 reaction mixtures were further characterized by LC-MS. The resultant fractions from the reaction were separated using a CombiFlash NextGen 300+ (Teledyne ISCO, Lincoln, NE) against a gradient of 100% methanol to 100% of a solution composed of 75% dichloromethane, 22% methanol, and 3% ammonium hydroxide over 55 min. Each peak was collected and dried, and the molecular weight of the fully saturated product was confirmed by LC-MS. This purified product was used to deliver human EPO mRNA.

Formulation of LNPs

The ionizable polyamine-lipid cores, prepared as described above, or DLin-MC3-DMA (MedChem Express, Monmouth Junction, NJ) were combined into an ethanol phase with cholesterol (Sigma-Aldrich), DOPE (Avanti, Alabaster, AL), and 1,2-dimyristoyl-*sn*-glycero-3-phosphoethanolamine-*N*-[methoxy(polyethylene glycol)-2000] (ammonium salt) (C14-PEG2000, Avanti) at molar ratios of 35:46.5:16:2.5, respectively, in a total volume of 112.5 μl. A separate aqueous phase was prepared consisting of 25 μg of luciferase (TriLink BioTechnologies, San Diego, CA) or EPO (TriLink BioTechnologies) mRNA and 10 mM citrate buffer (pH 3) in a total volume of 337.5 μl. All mRNA was N1-methyl-pseudo-U–capped with CleanCap technology offered by TriLink BioTechnologies. The ethanol and aqueous phases were combined through channels in a microfluidic device using a syringe pump as previously described (*39*). NPs were dialyzed against PBS for 2 hours before sterile filtration through syringe filters with 0.2-μm pores and stored at 4°C. JetPEI (Polyplus Transfection, New York, NY)–mRNA complexes were prepared according to manufacturer protocols with N/P = 7. All materials were prepared and handled ribonuclease-free throughout the synthesis, formulation, and characterization steps.

Nanoparticle characterization

For DLS and zeta potential measurements, 10 μl of each NP solution was combined with 1 ml of 1× PBS in 4-ml disposable cuvettes (for DLS) or zeta cuvettes (for zeta potential). Samples were run on a Zetasizer Nano (Malvern Instruments, Malvern, UK), and the reported measurements are averages ± SD from three runs. Surface ionization measurements to calculate the pK_a of each NP formulation were conducted as previously described (*36*). Aliquots of a buffered solution containing 150 mM sodium chloride, 20 mM sodium phosphate, 20 mM ammonium acetate, and 25 mM ammonium citrate were each adjusted to pH 2 to 12 in 0.5 increments. Two hundred microliters of each pH-adjusted solution was combined with 5 μl of each NP formulation in black 96-well plates in triplicate. TNS [6-(*p*-toluidinyl)naphthalene-2-sulfonic acid] was added to each well for a final TNS concentration of 6 μM, and the fluorescence intensity was read on an Infinite 200 Pro plate reader (Tecan, Morrisville, NC) (excitation, 322 nm; emission, 431 nm). The fluorescence intensity versus pH was plotted, and the pK_a was calculated to be the pH that corresponded to 50% protonation.

Encapsulation efficiencies were calculated using Quant-iT RiboGreen (Thermo Fisher Scientific, Waltham, MA) assays as previously described (*74*). Two microcentrifuge tubes with 350 μl of each NP solution were aliquoted, and 1% v/v Triton X-100 (Sigma-Aldrich) was added to one of the tubes. After 10 min, NPs (with and without Triton X-100) and RNA standards were plated in triplicate in black 96-well plates and the fluorescent RiboGreen reagent was added per manufacturer instructions. Fluorescence intensity was read on the plate reader (excitation, 490 nm; emission, 520 nm). To quantify encapsulation efficiency, background signal was subtracted from each well and triplicate wells were averaged. RNA content was quantified by comparing samples to the standard curve. Encapsulation efficiency was calculated according to the equation $\frac{B-A}{B} \times 100$, where A is the RNA content before treatment with Triton X-100 and B is the RNA content from samples treated with Triton X-100.

Animal experiments

All animal use was in accordance with the guidelines and approval from the Children's Hospital of Philadelphia's (CHOP) Institution of Animal Care and Use Committee. Balb/c mice were mated in our breeding colony (originally purchased from the Jackson Laboratory, Bar Harbor, ME) and maintained in the Laboratory Animal Facility of the Colket Translational Research Building at CHOP. Females of breeding age were paired with males and separated at 24 hours to achieve time-dated pregnant dams.

In vivo studies

Fetuses of time-dated pregnant Balb/c dams were injected at E16 as previously described (*75*). Briefly, under isoflurane anesthesia, a midline laparotomy was performed to expose the uterine horns. A dissecting microscope was used to identify the vitelline vein of each fetus, and a total volume of 5 μl (38.4 ng/μl mRNA) of the NP formulation was injected using an 80-μm beveled glass micropipette and an automated microinjector (Narishige IM-400 Electric Microinjector, Narishige International USA Inc., Amityville, NY). After successful injection, confirmed by visualizing clearance of the blood in the vein by the injectate, the uterus was returned to the peritoneal cavity and the abdomen was closed with a single layer of absorbable 4-0 polyglactin 910 suture.

Luciferase imaging

Mice were imaged either 4 or 24 hours after injection with NPs. Luciferase imaging was conducted on an IVIS (PerkinElmer, Waltham, MA). Ten minutes before imaging, dams were injected intraperitoneally with D-luciferin (150 mg/kg) and potassium salt (Biotium, Fremont, CA). Anesthetized mice were then placed supine into the IVIS, and luminescence signal was detected with a 60-s exposure time. Next, a midline laparotomy was performed to expose the uterine horns, and luciferase imaging was repeated. Dams were then sacrificed, and the fetuses were surgically extracted and placed in 1× PBS on ice. Fetuses were individually imaged by IVIS with 60-s exposure times. After imaging, the fetuses were dissected, and the liver, intestines, kidneys, heart, lungs, and brain were imaged by IVIS. Image analysis was conducted in the Living Image software (PerkinElmer). To quantify luminescent flux, a rectangular ROI was placed over each fetus or organ of interest, and an ROI of the same size was placed in an area without any luminescent signal in the same image. Normalized flux was calculated by dividing the total flux from the ROI over the fetus by the total flux from the background ROI. The representative IVIS images shown represent those images with quantified normalized luminescence in close proximity to the average value calculated for each LNP formulation.

GFP analysis

Mice were treated with LNP A-3 or B-4 with encapsulated GFP mRNA as described above. Fetuses were extracted after 24 hours and livers were collected for imaging and flow cytometry. For GFP imaging experiments, individual fetal livers were imaged using a fluorescent stereoscopic microscope (MZ716FA, Leica, Heerburg, Switzerland). Flow cytometry was used to quantify the percentage of cells in the liver that were GFP^+ following treatment. To do this, freshly dissected livers were immediately transferred to a dish containing ice-cold PBS, manually homogenized to create a single-cell suspension, and resuspended in FACS (fluorescence-activated cell sorting) staining buffer (1× PBS, 0.5% bovine serum albumin, and 0.2 mM EDTA, prepared in-house). After lysis of RBCs with ACK Lysing Buffer (Lonza Bioscience, Basel, Switzerland), liver cells were stained with anti-$CD45^-$APC (e-Bioscience Inc., San Diego, CA) for 30 min, washed three times, and resuspended in FACS buffer before running on a FACSAria flow cytometer (BD Biosciences, San Jose, CA). Gating was conducted to exclude $CD45^+$ lymphohematopoietic cells. Age-matched untreated mice served as a negative control for GFP^+ gate placement to determine the percentage of positive cells in livers from fetuses treated with LNPs.

Fetal survival and protein extraction

LNPs A-3, B-4, or DLin-MC3-DMA, PBS, or LPS/CpG (lipopolysaccharide/CG oligonucleotide) were injected into E16 fetuses via the vitelline vein. All of the fetuses in each dam ($n = 3$ dams) were injected. On E19, blood from the dams was collected retro-orbitally into blood collection tubes and centrifuged (10,000*g*, 10 min, 4°C), and plasma was harvested for cytokine analysis, liver enzymes, and complement activation. Next, fetuses were surgically removed to avoid any variability from the natural birthing process and poor parenting, and the pups were immediately evaluated for survival. Survival was assessed by observation of gross appearance, size, spontaneous movement, and a visible heartbeat. After assessing survival, pup livers were collected from a minimum of five injected fetuses for cytokine analysis and ALT/AST analysis (see below). The remaining injected fetuses were housed with foster female mice that had given birth to pups no more than 1 day before fostering.

Dam plasma and fetal livers were snap-frozen in dry ice and stored at −80°C until use. Frozen livers were cut on dry ice, and pieces were weighed using a Mettler-Toledo scale, thawed in 5 ml/g of tissue M-PER lysis buffer (Thermo Fisher Scientific) with cOmplete protease inhibitor cocktail (Roche, Basel, Switzerland), and immediately disrupted using the TissueLyzer II (Qiagen Inc., Germantown, MD) system with 5-mm steel beads (Qiagen Inc.) under 30-Hz frequency for 60 s; the homogenization process was repeated twice. Homogenized tissues were placed on ice for 30 min to allow complete lysis. Samples were centrifuged (2200*g*, 30 min, 4°C) and the supernatant was collected into new tubes. Total protein content in each sample was determined using the microBCA protein assay kit (Thermo Fisher Scientific) per manufacturer instructions.

Analysis of mRNA and LNP immunogenicity

Monocyte-derived human dendritic cells were used to evaluate the immunogenicity of mRNA without LNP carriers. Dendritic cells

were plated at 200,000 cells per well. Luciferase or EPO mRNA was complexed with TransIT-mRNA transfection reagent (Mirus Bio, Madison, WI) and added to hMD-DCs at 0.3 μg per well. The supernatant was collected 24 hours after transfection and evaluated for human IFN-α by an ELISA (Mabtech, 3425-1H-20, Cincinnati, OH) per manufacturer instructions.

For cytokine analysis in vivo, prepared fetal liver lysates and dam plasma samples were assessed for cytokine levels 3 days after LNP or PBS (control) injection using a 20–proinflammatory cytokine panel using Luminex technology. Plates were developed using the Milliplex assay builder (MilliporeSigma, Burlington, MA) and subjected to the manufacturer's quality control. Individual plates were used to analyze dam plasma samples or fetal livers. A standard curve for each plate was prepared by serially diluting the Milliplex Pro Mouse Cytokine Standard 20-Plex in the standard diluent (1:4 to 1:65,536). Plasma samples were diluted 1:20, and fetal liver samples were diluted 1:2 using the sample diluent, and 30 μl was transferred to the assay plates with prefilled capture antibodies. Each sample was plated in duplicate with five biological replicates per treatment group. The assay plates were incubated under orbital shaking (800 rpm) for 30 min and washed twice before the addition of biotinylated detection antibodies. Plates were incubated for 30 min (800 rpm), washed, and revealed with streptavidin-phycoerythrin for 10 min (800 rpm). Multiplex plates were run on the Bioplex 2200 system with a minimum of 50 beads analyzed per region. Each cytokine was assessed using a five-parameter regression algorithm (5-PL), with samples from LPS/GPC-injected mice as the positive control. Liver cytokine data were normalized to the protein concentration in the sample as determined by the microBCA assay.

Liver toxicity and complement system analysis

For liver toxicity studies, plasma samples from dams or fetal liver lysates were assessed for AST and ALT liver enzyme levels using AST or ALT colorimetric activity assay kits, respectively (Cayman Chemical, Ann Arbor, MI, USA) according to manufacturer recommendations at 3 days after LNP or PBS injection. Of note, because of the small fetal size and limited fetal serum availability, fetal cytokine production and fetal liver enzymes were assessed in fetal liver lysates rather than serum. Thus, fetal AST/ALT data were normalized to the protein concentration in the sample as determined by the microBCA assay. Complement system activation from plasma collected from the dams was assessed using Immunotag Mouse C3 (complement C3) and Immunotag Mouse C4 (complement C4) ELISA kits (G-Biosciences, St. Louis, MO, USA) per manufacturer instructions. We were unable to assess complement system activation directly from fetal plasma due to the low volume of blood present in fetuses at this gestational age.

Quantification of EPO production

The ionizable lipids used in LNP formulations A-3 and B-4 were purified as described above. LNPs were prepared with human EPO mRNA (TriLink BioTechnologies) and injected into E16 fetuses via the vitelline vein. Fetal livers were harvested at 4 and 24 hours after injection and kept on ice during processing. Livers were rinsed three times with 1× PBS to remove excess blood and were then homogenized in 5 ml of 1× PBS using 15-ml tissue grinders (Thermo Fisher Scientific). Lysates were brought through two repeated overnight freeze-thaw cycles to break up cell membranes. After the final thaw, processed liver samples were centrifuged (5 min, 5000*g*) and the supernatant was collected for analysis. EPO content in the supernatant was quantified by ELISA using the Human Erythropoietin Quantikine IVD ELISA Kit (R&D Systems, Minneapolis, MN) per manufacturer recommendations. Data shown are average and SEM of EPO concentrations from at least three fetuses injected in each experimental group.

Statistical analysis

All luciferase quantifications represent the mean and SEM of the normalized luminescence signal acquired from at least three fetuses per treatment group depending on the number of fetuses in each dam (Figs. 3 and 4, minimum $n = 3$). The means were compared by one-way analysis of variance (ANOVA) with post hoc Tukey-Kramer. The mean EPO concentrations (Fig. 5) were compared by two-way ANOVA across both injection volume and LNP formulation, and error bars are SEM. Liver enzyme, complement activation, and cytokine analysis data represent mean and SEM, and statistical analysis was done using two-way ANOVA with post hoc Tukey-Kramer (Fig. 6). Outliers were detected using Grubbs' test and were removed from analysis.

SUPPLEMENTARY MATERIALS

Supplementary material for this article is available at http://advances.sciencemag.org/cgi/content/full/7/3/eaba1028/DC1

View/request a protocol for this paper from *Bio-protocol*.

REFERENCES AND NOTES

1. Y. M. D. Lo, M. S. C. Tein, T. K. Lau, C. J. Haines, T. N. Leung, P. M. K. Poon, J. S. Wainscoat, P. J. Johnson, A. M. Z. Chang, N. M. Hjelm, Quantitative analysis of fetal DNA in maternal plasma and serum: Implications for noninvasive prenatal diagnosis. *Am. J. Hum. Genet.* **62**, 768–775 (1998).
2. D. W. Bianchi, J. M. Williams, L. M. Sullivan, F. W. Hanson, K. W. Klinger, A. P. Shuber, PCR quantitation of fetal cells in maternal blood in normal and aneuploid pregnancies. *Am. J. Hum. Genet.* **61**, 822–829 (1997).
3. C. R. Ferreira, W. A. Gahl, Lysosomal storage diseases. *Transl. Sci. Rare Dis.* **2**, 1–71 (2017).
4. G. Massaro, C. N. Z. Mattar, A. M. S. Wong, E. Sirka, S. M. K. Buckley, B. R. Herbert, S. Karlsson, D. P. Perocheau, D. Burke, S. Heales, A. Richard-Iondt, S. Brandner, M. Huebecker, D. A. Priestman, F. M. Platt, K. Mills, A. Biswas, J. D. Cooper, J. K. Y. Chan, S. H. Cheng, S. N. Waddington, A. A. Rahim, Fetal gene therapy for neurodegenerative disease of infants. *Nat. Med.* **24**, 1317–1323 (2018).
5. D. Alapati, W. J. Zacharias, H. A. Hartman, A. C. Rossidis, J. D. Stratigis, N. J. Ahn, B. Coons, S. Zhou, H. Li, K. Singh, J. Katzen, Y. Tomer, A. C. Chadwick, K. Musunuru, M. F. Beers, E. E. Morrisey, W. H. Peranteau, In utero gene editing for monogenic lung disease. *Sci. Transl. Med.* **11**, eaav8375 (2019).
6. S. DeWeerdt, Prenatal gene therapy offers the earliest possible cure. *Nature* **564**, S6–S8 (2018).
7. G. Almeida-porada, A. Atala, C. D. Porada, In utero stem cell transplantation and gene therapy: Rationale, history, and recent advances toward clinical application. *Mol. Ther. Clin. Dev.* **5**, 16020 (2016).
8. D. Songdej, C. Babbs, D. Higgs; BHFS International Consortium, An international registry of survivors with Hb Bart's hydrops fetalis syndrome. *Blood* **129**, 1251–1259 (2017).
9. D. Chui, J. Waye, Hydrops fetalis caused by α-thalassemia: An emerging health care problem. *Blood* **91**, 2213–2222 (1998).
10. B. Connolly, C. Isaacs, L. Cheng, K. H. Asrani, R. R. Subramanian, SERPINA1 mRNA as a treatment for alpha-1 antitrypsin deficiency. *J. Nucleic Acids.* **2018**, 8247935 (2018).
11. J. F. Apgar, J.-P. Tang, P. Singh, N. Balasubramanian, J. Burke, M. R. Hodges, M. A. Lasaro, L. Lin, B. L. Miliard, K. Moore, L. S. Jun, S. Sobolov, A. K. Wilkins, X. Gao, Quantitative systems pharmacology model of hUGT1A1-modRNA encoding for the UGT1A1 enzyme to treat crigler-najjar syndrome type 1. *CPT Pharmacometrics Syst. Pharmacol.* **7**, 404–412 (2018).
12. D. S. Roseman, T. Khan, F. Rajas, L. S. Jun, K. H. Asrani, C. Isaacs, J. D. Farelli, R. R. Subramanian, G6PC mRNA therapy positively regulates fasting blood glucose and decreases liver abnormalities in a mouse model of glycogen storage disease 1a. *Mol. Ther.* **26**, 814–821 (2018).
13. F. Derosa, B. Guild, S. Karve, L. Smith, K. Love, J. R. Dorkin, K. J. Kauffman, J. Zhang, B. Yahalom, D. G. Anderson, M. W. Heartlein, Therapeutic efficacy in a hemophilia B model using a biosynthetic mRNA liver depot system. *Gene Ther.* **23**, 699–707 (2016).

14. Z. Trepotec, E. Lichtenegger, C. Plank, M. K. Aneja, C. Rudolph, Delivery of mRNA therapeutics for the treatment of hepatic diseases. *Mol. Ther.* **27**, 794–802 (2019).
15. A. S. Ricciardi, R. Bahal, J. S. Farrelly, E. Quijano, A. H. Bianchi, V. L. Luks, R. Putman, F. López-giráldez, S. Co, E. Song, Y. Liu, W. Hsieh, D. H. Ly, D. H. Stitelman, P. M. Glazer, W. M. Saltzman, In utero nanoparticle delivery for site-specific genome editing. *Nat. Commun.* **9**, 2481 (2018).
16. A. C. Rossidis, J. D. Stratigis, A. C. Chadwick, H. A. Hartman, N. J. Ahn, H. Li, K. Singh, B. E. Coons, L. Li, W. Lv, W. Zoltick, D. Alapati, W. Zacharias, R. Jain, E. E. Morrisey, K. Musunuru, W. H. Peranteau, In utero CRISPR-mediated therapeutic editing of metabolic genes. *Nat. Med.* **24**, 1513–1518 (2018).
17. M. G. Davey, J. S. Riley, A. Andrews, A. Tyminski, M. Limberis, J. E. Pogoriler, E. Partridge, A. Olive, H. L. Hedrick, A. W. Flake, W. H. Peranteau, Induction of immune tolerance to foreign protein via adeno-associated viral vector gene transfer in mid-gestation fetal sheep. *PLOS One.* **12**, e0171132 (2017).
18. N. Pardi, M. J. Hogan, F. W. Porter, D. Weissman, mRNA vaccines—A new era in vaccinology. *Nat. Rev. Drug Discov.* **17**, 261–279 (2018).
19. R. S. Riley, C. H. June, R. Langer, M. J. Mitchell, Delivery technologies for cancer immunotherapy. *Nat. Rev. Drug Discov.* **18**, 175–196 (2019).
20. K. A. Hajj, K. A. Whitehead, Tools for translation: Non-viral materials for therapeutic mRNA delivery. *Nat. Rev. Mater.* **2**, 17056 (2017).
21. P. P. G. Guimaraes, R. Zhang, R. Spektor, M. Tan, A. Chung, M. M. Billingsley, R. El-mayta, R. S. Riley, L. Wang, J. M. Wilson, M. J. Mitchell, Ionizable lipid nanoparticles encapsulating barcoded mRNA for accelerated *in vivo* delivery screening. *J. Control. Release* **316**, 404–417 (2019).
22. O. S. Fenton, K. N. Olafson, P. S. Pillai, M. J. Mitchell, R. Langer, Advances in biomaterials for drug delivery. *Adv. Mater.* **30**, 1705328 (2018).
23. L. E. McClain, A. W. Flake, In utero stem cell transplantation and gene therapy: Recent progress and the potential for clinical application. *Best Pract. Res. Clin. Obstet. Gynaecol.* **31**, 88–98 (2016).
24. J. L. Roybal, M. T. Santore, A. W. Flake, Stem cell and genetic therapies for the fetus. *Semin. Fetal Neonatal Med.* **15**, 46–51 (2010).
25. R. Karda, S. M. K. Buckley, C. N. Mattar, J. Ng, G. Massaro, M. A. Kurian, J. Baruteau, P. Gissen, J. K. Y. Chan, C. Bacchelli, S. N. Waddington, A. A. Rahim, Perinatal systemic gene delivery using adeno-associated viral vectors. *Front. Mol. Neurosci.* **7**, 89 (2014).
26. S. J. Howe, M. R. Mansour, K. Schwarzwaelder, C. Bartholomae, M. Hubank, H. Kempski, M. H. Brugman, K. Pike-overzet, S. J. Chatters, D. De Ridder, K. C. Gilmour, S. Adams, S. I. Thornhill, K. L. Parsley, F. J. T. Staal, R. E. Gale, D. C. Linch, J. Bayford, L. Brown, M. Quaye, C. Kinnon, P. Ancliff, D. K. Webb, M. Schmidt, C. von Kalle, H. B. Gaspar, A. J. Thrasher, Insertional mutagenesis combined with acquired somatic mutations causes leukemogenesis following gene therapy of SCID-X1 patients. *J. Clin. Invest.* **118**, 3143–3150 (2008).
27. A. J. Mukalel, R. S. Riley, R. Zhang, M. J. Mitchell, Nanoparticles for nucleic acid delivery: Applications in cancer immunotherapy. *Cancer Lett.* **458**, 102–112 (2019).
28. S. B. Fournier, J. N. D'Errico, P. A. Stapleton, Engineered nanomaterial applications in perinatal therapeutics. *Pharmacol. Res.* **130**, 36–43 (2018).
29. F. Danhier, E. Ansorena, J. M. Silva, R. Coco, A. Le Breton, V. Préat, PLGA-based nanoparticles: An overview of biomedical applications. *J. Control. Release* **161**, 505–522 (2012).
30. F. Alexis, E. Pridgen, L. K. Molnar, O. C. Farokhzad, Factors affecting the clearance and biodistribution of polymeric nanoparticles. *Mol. Pharm.* **5**, 505–515 (2008).
31. H. K. Mandl, E. Quijano, H. W. Suh, E. Sparago, S. Oeck, M. Grun, P. M. Glazer, W. M. Saltzman, Optimizing biodegradable nanoparticle size for tissue-specific delivery. *J. Control. Release* **314**, 92–101 (2019).
32. W. Huang, C. Zhang, Tuning the size of poly(lactic-co-glycolic acid) (PLGA) nanoparticles fabricated by nanoprecipitation. *Biotechnol. J.* **13**, (2018).
33. M. C. Operti, Y. Dölen, J. Keulen, E. A. W. van Dinther, C. G. Figdor, O. Tagit, Microfluidics-assisted size tuning and biological evaluation of PLGA particles. *Pharmaceutics* **11**, 590 (2019).
34. K. J. Kauffman, J. R. Dorkin, J. H. Yang, M. W. Heartlein, F. Derosa, F. F. Mir, O. S. Fenton, D. G. Anderson, Optimization of lipid nanoparticle formulations for mRNA delivery in vivo with fractional factorial and definitive screening designs. *Nano Lett.* **15**, 7300–7306 (2015).
35. M. A. Oberli, A. M. Reichmuth, J. R. Dorkin, M. J. Mitchell, O. S. Fenton, A. Jaklenec, D. G. Anderson, R. Langer, D. Blankschtein, Lipid nanoparticle assisted mRNA delivery for potent cancer immunotherapy. *Nano Lett.* **17**, 1326–1335 (2017).
36. K. A. Hajj, R. L. Ball, S. B. Deluty, S. R. Singh, D. Strelkova, C. M. Knapp, K. A. Whitehead, Branched-tail lipid nanoparticles potently deliver mRNA in vivo due to enhanced ionization at endosomal pH. *Small* **15**, e1805097 (2019).
37. T. M. Allen, P. R. Cullis, Liposomal drug delivery systems: From concept to clinical applications. *Adv. Drug Deliv. Rev.* **65**, 36–48 (2013).
38. I. Zuhorn, U. Bakowsky, E. Polushkin, W. Visser, M. Stuart, J. Engberts, D. Hoekstra, Nonbilayer phase of lipoplex-membrane mixture determines endosomal escape of genetic cargo and transfection efficiency. *Mol. Ther.* **11**, 801–810 (2005).
39. D. Chen, K. T. Love, Y. Chen, A. A. Eltoukhy, C. Kastrup, G. Sahay, A. Jeon, Y. Dong, K. A. Whitehead, D. G. Anderson, Rapid discovery of potent siRNA-containing lipid nanoparticles enabled by controlled microfluidic formulation. *J. Am. Chem. Soc.* **134**, 6948–6951 (2012).
40. K. T. Love, K. P. Mahon, G. Christopher, K. A. Whitehead, W. Querbes, J. R. Dorkin, J. Qin, W. Cantley, L. L. Qin, M. Frank-kamenetsky, K. N. Yip, R. Alvarez, D. W. Y. Sah, A. de Fougerolles, K. Fitzgerald, V. Koteliansky, A. Akinc, R. Langer, D. G. Anderson, Lipid-like materials for low-dose, in vivo gene silencing. *Proc. Natl. Acad. Sci.* **107**, 1864–1869 (2010).
41. M. Jayaraman, S. M. Ansell, B. L. Mui, Y. K. Tam, J. Chen, X. Du, D. Butler, L. Eltepu, S. Matsuda, J. K. Narayanannair, K. G. Rajeev, I. M. Hafez, A. Akinc, M. A. Maier, M. A. Tracy, P. R. Cullis, T. D. Madden, M. Manoharan, M. J. Hope, Maximizing the potency of siRNA lipid nanoparticles for hepatic gene silencing in vivo. *Angew. Chem. Int. Ed. Engl.* **51**, 8529–8533 (2012).
42. K. A. Whitehead, J. R. Dorkin, A. J. Vegas, P. H. Chang, O. Veiseh, J. Matthews, O. S. Fenton, Y. Zhang, K. T. Olejnik, V. Yesilyurt, D. Chen, S. Barros, B. Klebanov, T. Novobrantseva, R. Langer, D. G. Anderson, Degradable lipid nanoparticles with predictable in vivo siRNA delivery activity. *Nat. Commun.* **5**, 4277 (2014).
43. O. M. Swartley, J. F. Foley, D. P. Livingston III, J. M. Cullen, S. A. Elmore, Histology atlas of the developing mouse hepatobiliary hemolymphatic vascular system with emphasis on embryonic days 11.5-18.5 and early postnatal development. *Toxicol. Pathol.* **44**, 705–725 (2016).
44. S. M. Sarett, T. A. Werfel, L. Lee, M. A. Jackson, K. V. Kilchrist, D. Brantley-sieders, C. L. Duvall, Lipophilic siRNA targets albumin in situ and promotes bioavailability, tumor penetration, and carrier-free gene silencing. *Proc. Natl. Acad. Sci. U.S.A.* **114**, E6490–E6497 (2017).
45. K. Garber, Alnylam launches era of RNAi drugs. *Nat. Biotechnol.* **36**, 777–778 (2018).
46. D. Adams, A. Gonzalez-Duarte, W. D. O'Riordan, C.-C. Yang, M. Ueda, A. V. Kristen, I. Tournev, H. H. Schmidt, T. Coelho, J. L. Berk, K.-P. Lin, G. Vita, S. Attarian, V. Planté-Bordeneuve, M. M. Mezei, J. M. Campistol, J. Buades, T. H. Brannagan III, B. J. Kim, J. Oh, Y. Parman, Y. Sekijima, P. N. Hawkins, S. D. Solomon, M. Polydefkis, P. J. Dyck, P. J. Gandhi, S. Goyal, J. Chen, A. L. Strahs, S. V. Nochur, M. T. Sweetser, P. P. Garg, A. K. Vaishnaw, J. A. Gollob, O. B. Suhr, Patisiran, an RNAi therapeutic, for hereditary transthyretin amyloidosis. *N. Engl. J. Med.* **379**, 11–21 (2018).
47. X. Zhang, V. Goel, G. J. Robbie, Pharmacokinetics of Patisiran, the first approved RNA interference therapy in patients with hereditary transthyretin-mediated amyloidosis. *J. Clin. Pharmacol.* **60**, 573–585 (2019).
48. A. A. Sidi, P. Ohana, S. Benjamin, M. Shalev, J. H. Ransom, D. Lamm, A. Hochberg, I. Leibovitch, Phase I/II marker lesion study of intravesical BC-819 DNA plasmid in H19 over expressing superficial bladder cancer refractory to bacillus calmette-guerin. *J. Urol.* **180**, 2379–2383 (2008).
49. K. Bahl, J. J. Senn, O. Yuzhakov, A. Bulychev, L. A. Brito, K. J. Hassett, M. E. Laska, M. Smith, Ö. Almarsson, J. Thompson, A. M. Ribeiro, M. Watson, T. Zaks, G. Ciaramella, Preclinical and clinical demonstration of immunogenicity by mRNA vaccines against H10N8 and H7N9 influenza viruses. *Mol. Ther.* **25**, 1316–1327 (2017).
50. O. F. Khan, E. W. Zaia, S. Jhunjhunwala, W. Xue, W. Cai, D. S. Yun, C. M. Barnes, J. E. Dahlman, Y. Dong, J. M. Pelet, M. J. Webber, J. K. Tsosie, T. E. Jacks, R. Langer, D. G. Anderson, Dendrimer-inspired nanomaterials for the in vivo delivery of siRNA to lung vasculature. *Nano Lett.* **15**, 3008–3016 (2015).
51. K. De Filippo, R. B. Henderson, M. Laschinger, N. Hogg, Neutrophil chemokines KC and macrophage-inflammatory protein-2 are newly synthesized by tissue macrophages using distinct TLR signaling pathways. *J. Immunol.* **180**, 4308–4315 (2008).
52. H. Watanabe, K. Numata, T. Ito, K. Takagi, A. Matsukawa, Innate immune response in Th1- and Th2-dominant mouse strains. *Shock* **22**, 460–466 (2004).
53. S. M. Winkler, M. R. Harrison, P. B. Messersmith, Biomaterials in fetal surgery. *Biomater. Sci.* **7**, 3092–3109 (2019).
54. Committee on Genetics, Committee opinion no. 690 summary: Carrier screening in the age of genomic medicine. *Obstet. Gynecol.* **129**, e35–e40 (2017).
55. A. Safary, M. A. Khiavi, R. Mousavi, J. Barar, M. A. Rafi, Enzyme replacement therapies: What is the best option? *Bioimpacts* **8**, 153–157 (2018).
56. J. A. Gorzelany, M. P. de Souza, Protein replacement therapies for rare diseases: A breeze for regulatory approval? *Sci. Transl. Med.* **5**, 178fs10 (2013).
57. S. Ramaswamy, N. Tonnu, K. Tachikawa, P. Limphong, J. B. Vega, P. P. Karmali, P. Chivukula, I. M. Verma, Systemic delivery of factor IX messenger RNA for protein replacement therapy. *Proc. Natl. Acad. Sci.* **114**, E1941–E1950 (2017).
58. B. Truong, G. Allegri, X.-B. Liu, K. E. Burke, X. Zhu, S. D. Cederbaum, J. Häberle, P. G. V. Martini, G. S. Lipshutz, Lipid nanoparticle-targeted mRNA therapy as a treatment for the inherited metabolic liver disorder arginase deficiency. *Proc. Natl. Acad. Sci.* **116**, 21150–21159 (2019).

59. C. P. Gheorghe, N. Boring, L. Mann, R. Donepudi, S. M. Lopez, S. P. Chauhan, V. Bhandari, K. J. Moise Jr., A. Johnson, R. Papanna, Neonatal outcomes and maternal characteristics in monochorionic diamniotic twin pregnancies: Uncomplicated versus twin-to-twin transfusion syndrome survivors after fetoscopic laser surgery. *Fetal Diagn. Ther.* **47**, 165–170 (2020).
60. M. L. Kovler, E. B. Jelin, Fetal intervention for congenital diaphragmatic hernia. *Semin. Pediatr. Surg.* **28**, 150818 (2019).
61. N. S. Adzick, E. A. Thom, C. Y. Spong, J. W. Brock, P. K. Burrows, M. P. Johnson, L. J. Howell, J. A. Farrell, M. E. Dabrowiak, L. N. Sutton, N. Gupta, D. Ph, N. B. Tulipan, M. E. D'Alton, D. L. Farmer; MOMS Investigators, A randomized trial of prenatal versus postnatal repair of myelomeningocele. *N. Engl. J. Med.* **364**, 993–1004 (2011).
62. S. Montazersaheb, M. S. Hejazi, H. N. Charoudeh, Potential of peptide nucleic acids in future therapeutic applications. *Adv. Pharm. Bull.* **8**, 551–563 (2018).
63. M. M. Boelig, A. G. Kim, J. D. Stratigis, L. E. Mcclain, H. Li, A. W. Flake, W. H. Peranteau, The intravenous route of injection optimizes engraftment and survival in the murine model of in utero hematopoietic cell transplantation. *Biol. Blood Marrow Transplant.* **22**, 991–999 (2016).
64. P. Shangaris, S. P. Loukogeorgakis, S. Subramaniam, C. Flouri, L. H. Jackson, W. Wang, M. P. Blundell, S. Liu, S. Eaton, N. Bakhamis, D. L. Ramachandra, P. Maghsoudlou, L. Urbani, S. N. Waddington, A. Eddaoudi, J. Archer, M. N. Antoniou, D. J. Stuckey, M. Schmidt, A. J. Thrasher, T. M. Ryan, P. De Coppi, A. L. David, In utero gene therapy (IUGT) using GLOBE lentiviral vector phenotypically corrects the heterozygous humanised mouse model and its progress can be monitored using MRI techniques. *Sci. Rep.* **9**, 11592 (2019).
65. F. Prefumo, A. Fichera, N. Fratelli, E. Sartori, Fetal anemia: Diagnosis and management. *Best Pr. Res Clin Obs. Gynaecol.* **58**, 2–14 (2019).
66. N. Abbasi, J.-A. Johnson, G. Ryan, Fetal anemia. *Ultrasound Obstet. Gynecol.* **50**, 145–153 (2017).
67. A. Mejaddam, M. A. Hornick, P. E. McGovern, H. D. Baumgarten, K. M. Lawrence, A. C. Rossidis, G. Hwang, K. Young, O. Abdulmalik, E. A. Partridge, W. H. Peranteau, M. G. Davey, A. W. Flake, Erythropoietin prevents anemia and transfusions in extremely premature lambs supported by an EXTrauterine environment for neonatal development (EXTEND). *Fetal Diagn. Ther.* **46**, 231–237 (2019).
68. Q.-H. Nguyen, R. G. Witt, B. Want, C. Eikani, J. Shea, L. K. Smith, G. Boyle, J. Cadaoas, R. Sper, J. D. MacKenzie, S. Villeda, T. MacKenzie, Tolerance induction and microglial engraftment after fetal therapy without conditioning in mice with mucopolysaccharidosis type VII. *Sci. Transl. Med.* **12**, eaay8980 (2020).
69. C.-C. Qin, Y.-N. Liu, Y. Hu, Y. Yang, Z. Chen, Macrophage inflammatory protein-2 as mediator of inflammation in acute liver injury. *World J. Gastroenterol.* **23**, 3043–3052 (2017).
70. M. Sedic, J. J. Senn, A. Lynn, M. Laska, M. Smith, S. J. Platz, J. Bolen, S. Hoge, A. Bulychev, E. Jacquinet, V. Bartlett, P. F. Smith, Safety evaluation of lipid nanoparticle–formulated modified mRNA in the sprague-dawley rat and cynomolgus monkey. *Vet. Pathol.* **55**, 341–354 (2018).
71. S. Sabnis, E. S. Kumarasinghe, T. Salerno, C. Mihai, T. Ketova, J. J. Senn, A. Lynn, A. Bulychev, I. McFadyen, J. Chan, Ö. Almarsson, M. G. Stanton, K. E. Benenato, A novel amino lipid series for mRNA delivery: Improved endosomal escape and sustained pharmacology and safety in non-human primates. *Mol. Ther.* **26**, 1509–1519 (2018).
72. J. A. Kulkarni, P. R. Cullis, R. van der Meel, Lipid nanoparticles enabling gene therapies: From concepts to clinical utility. *Nucleic Acid Ther.* **28**, 146–157 (2018).
73. E. M. Kreger, S. T. Singer, R. G. Witt, N. Sweeters, B. Lianoglou, A. Lal, T. C. Mackenzie, E. Vichinsky, Favorable outcomes after in utero transfusion in fetuses with alpha thalassemia major: A case series and review of the literature. *Prenat. Diagn.* **36**, 1242–1249 (2016).
74. J. Heyes, L. Palmer, K. Bremner, I. Maclachlan, Cationic lipid saturation influences intracellular delivery of encapsulated nucleic acids. *J. Control. Release* **107**, 276–287 (2005).
75. N. Ahn, J. D. Stratigis, B. E. Coons, A. W. Flake, H.-D. Nah-Cederquist, W. H. Peranteau, Intravenous and intra-amniotic in utero transplantation in the murine model. *J. Vis. Exp.* **140**, 58047 (2018).

Acknowledgments: We acknowledge the Children's Hospital of Philadelphia Small Animal Imaging Facility for maintenance of the IVIS. **Funding:** Research reported in this publication was supported in part by the Institute for Translational Medicine and Therapeutics (ITMAT) Transdisciplinary Program in Translational Medicine and Therapeutics. This work was also supported by the U.S. National Institutes of Health (NIH) Director's New Innovator Awards (DP2 TR002776 to M.J.M. and DP2HL152427 to W.H.P.), NIH 1R01DK123049-01 to W.H.P. and M.J.M., and a Burroughs Wellcome Fund Career Award at the Scientific Interface (CASI) to M.J.M. R.S.R. was supported by an NIH T32 training grant (T32HL007954) and an NIH NCI F32 fellowship (1F32CA24347-01A1). M.V.K. was supported by an NIH NHLBI F32 fellowship (F32HL143861). M.M.B. was supported by a Tau Beta Pi Fellowship. **Author contributions:** R.S.R., M.V.K., and M.M.B. contributed to the experimental design, data collection, analysis and interpretation, and writing of this manuscript. M.-G.A. and D.W. contributed to the design, execution, and analysis of the immunotoxicity studies and critically reviewed the manuscript. R.Z. assisted with nanoparticle characterization, and B.W., A.Y.C., and S.K.B. assisted with IVIS imaging. P.W.Z. contributed to the project design and manuscript review. H.L. assisted with the flow cytometry experiments and analysis. M.J.M. and W.H.P. equally contributed to the direction of the project and writing of this manuscript. **Competing interests:** D.W. is an inventor on several patents related to this work filed by the Trustees of the University of Pennsylvania (11/990,646; 13/585,517; 13/839,023; 13/839,155; 14/456,302; 15/339,363; and 16/299,202). M.J.M. is an inventor on a patent related to this work filed by the Trustees of the University of Pennsylvania (PCT/US20/56252). The authors declare that they have no other competing interests. **Data and materials availability:** All data needed to evaluate the conclusions in the paper are present in the paper and/or the Supplementary Materials. All data and materials are stored at the University of Pennsylvania and Children's Hospital of Philadelphia facilities in the Mitchell and Peranteau laboratories. Additional data related to this paper may be requested from the corresponding authors: M.J.M. (mjmitch@seas.upenn.edu) and/or W.H.P. (peranteauw@email.chop.edu).

Submitted 18 November 2019
Accepted 20 November 2020
Published 13 January 2021
10.1126/sciadv.aba1028

Citation: R. S. Riley, M. V. Kashyap, M. M. Billingsley, B. White, M.-G. Alameh, S. K. Bose, P. W. Zoltick, H. Li, R. Zhang, A. Y. Cheng, D. Weissman, W. H. Peranteau, M. J. Mitchell, Ionizable lipid nanoparticles for in utero mRNA delivery. *Sci. Adv.* **7**, eaba1028 (2021).

Ionizable lipid nanoparticles for in utero mRNA delivery

Rachel S. Riley, Meghana V. Kashyap, Margaret M. Billingsley, Brandon White, Mohamad-Gabriel Alameh, Sourav K. Bose, Philip W. Zoltick, Hiaying Li, Rui Zhang, Andrew Y. Cheng, Drew Weissman, William H. Peranteau and Michael J. Mitchell

Sci Adv **7** (3), eaba1028.
DOI: 10.1126/sciadv.aba1028